The Astrophysical Journal, 718:86–104, 2010 July 20 doi:10.1088/0004-637X/718/1/86

THE 10k zCOSMOS: MORPHOLOGICAL TRANSFORMATION OF GALAXIES IN THE GROUP ENVIRONMENT SINCE $z \sim 1$*

K. Kovač[1], S. J. Lilly[1], C. Knobel[1], M. Bolzonella[2], A. Iovino[3], C. M. Carollo[1], C. Scarlata[4], M. Sargent[5], O. Cucciati[6], G. Zamorani[2], L. Pozzetti[2], L. A. M. Tasca[6,7], M. Scodeggio[7], P. Kampczyk[1], Y. Peng[1], P. Oesch[1], E. Zucca[2], A. Finoguenov[8], T. Contini[9], J.-P. Kneib[6], O. Le Fèvre[6], V. Mainieri[10], A. Renzini[11], S. Bardelli[2], A. Bongiorno[8], K. Caputi[1], G. Coppa[2], S. de la Torre[3,6,7], L. de Ravel[6], P. Franzetti[7], B. Garilli[7], F. Lamareille[9], J.-F. Le Borgne[9], V. Le Brun[6], C. Maier[1], M. Mignoli[2], R. Pello[9], E. Perez Montero[9], E. Ricciardelli[12], J. D. Silverman[1], M. Tanaka[10], L. Tresse[6], D. Vergani[2], U. Abbas[6,13], D. Bottini[7], A. Cappi[2], P. Cassata[6,14], A. Cimatti[15], M. Fumana[7], L. Guzzo[3], A. M. Koekemoer[16], A. Leauthaud[17], D. Maccagni[7], C. Marinoni[18], H. J. McCracken[19], P. Memeo[7], B. Meneux[8,20], C. Porciani[1,21], R. Scaramella[22], and N. Z. Scoville[23]

[1] Institute of Astronomy, ETH Zürich, CH-8093, Zürich, Switzerland
[2] INAF Osservatorio Astronomico di Bologna, via Ranzani 1, I-40127, Bologna, Italy
[3] INAF Osservatorio Astronomico di Brera, Milan, Italy
[4] Spitzer Science Center, 314-6 Caltech, Pasadena, CA 91125, USA
[5] Max-Planck-Institut für Astronomie, Königstuhl 17, D-69117 Heidelberg, Germany
[6] Laboratoire d'Astrophysique de Marseille, Marseille, France
[7] INAF-IASF Milano, Milan, Italy
[8] Max-Planck-Institut für extraterrestrische Physik, D-84571 Garching, Germany
[9] Laboratoire d'Astrophysique de Toulouse-Tarbes, Universite de Toulouse, CNRS, 14 Avenue Edouard Belin, F-31400 Toulouse, France
[10] European Southern Observatory, Karl-Schwarzschild- Strasse 2, Garching, D-85748, Germany
[11] INAF-Osservatorio Astronomico di Padova, Padova, Italy
[12] Dipartimento di Astronomia, Universita di Padova, Padova, Italy
[13] INAF Osservatorio Astronomico di Torino, Strada Osservatorio 20, I-10025 Pino Torinese, Torino, Italy
[14] Department of Astronomy, University of Massachusetts, Amherst, MA 01003, USA
[15] Dipartimento di Astronomia, Universitá di Bologna, via Ranzani 1, I-40127, Bologna, Italy
[16] Space Telescope Science Institute, 3700 San Martin Drive, Baltimore, MD 21218, USA
[17] Physics Division, MS 50 R5004, Lawrence Berkeley National Laboratory, 1 Cyclotron Rd., Berkeley, CA 94720, USA
[18] Centre de Physique Theorique, Marseille, Marseille, France
[19] Institut d'Astrophysique de Paris, UMR 7095 CNRS, Université Pierre et Marie Curie, 98 bis Boulevard Arago, F-75014 Paris, France
[20] Universitäts-Sternwarte, Scheinerstrasse 1, Munich D-81679, Germany
[21] Argelander-Institut für Astronomie, Auf dem Hügel 71, D-53121 Bonn, Germany
[22] INAF, Osservatorio di Roma, Monteporzio Catone (RM), Italy
[23] California Institute of Technology, MS 105-24, Pasadena, CA 91125, USA
Received 2009 August 24; accepted 2010 March 3; published 2010 June 28

ABSTRACT

We study the evolution of galaxies inside and outside of the group environment since $z = 1$ using a large well-defined set of groups and galaxies from the zCOSMOS-bright redshift survey in the COSMOS field. The fraction of galaxies with early-type morphologies increases monotonically with M_B luminosity and stellar mass and with cosmic epoch. It is higher in the groups than elsewhere, especially at later epochs. The emerging environmental effect is superposed on a strong global mass-driven evolution, and at $z \sim 0.5$ and $\log(M_*/M_\odot) \sim 10.2$, the "effect" of the group environment is equivalent to (only) about 0.2 dex in stellar mass or 2 Gyr in time. The stellar mass function of galaxies in groups is enriched in massive galaxies. We directly determine the transformation rates from late to early morphologies, and for transformations involving color and star formation indicators. The transformation rates are systematically about twice as high in the groups as outside, or up to three to four times higher correcting for infall and the appearance of new groups. The rates reach values as high as 0.3–0.7 Gyr^{-1} in the groups (for masses around the crossing mass $10^{10.5}\,M_\odot$), implying transformation timescales of 1.4–3 Gyr, compared with less than 0.2 Gyr^{-1}, i.e., timescales >5 Gyr, outside of groups. All three transformation rates decrease at higher stellar masses, and must also decrease at lower masses below $10^{10}\,M_\odot$ which we cannot probe well. The rates involving color and star formation are consistently higher than those for morphology, by a factor of about 50%. Our conclusion is that the transformations that drive the evolution of the overall galaxy population since $z \sim 1$ must occur at a rate two to four times higher in groups than outside of them.

Key words: galaxies: clusters: general – galaxies: evolution – galaxies: high-redshift – galaxies: luminosity function, mass function – galaxies: structure

Online-only material: color figures

1. INTRODUCTION

Galaxies exhibit a range of morphologies that reflect, at least in part, basic structural differences, such as the presence of disks, spheroids, and bars, as well as differences in the visibility of spiral arms due to, for instance, the rate of star formation.

* Based on observations obtained at the European Southern Observatory (ESO) Very Large Telescope (VLT), Paranal, Chile, as part of the Large Program 175.A-0839 (the zCOSMOS Spectroscopic Redshift Survey).

The commonly used morphological classification follows the Hubble sequence of elliptical, S0, spiral, barred spiral, and irregular galaxies with various subclasses (Hubble 1926, 1936; Sandage 1961). Galaxy morphology is undoubtedly a complex phenomenon reflecting different physical processes operating within and around a given galaxy. There are several underlying correlations involving morphology. At least up to $z \sim 1$, early-type galaxies are observed to be redder, older, more luminous, and more massive than spiral and irregular galaxies (e.g., Bell et al. 2004; Bundy et al. 2006; Pozzetti et al. 2009; Bolzonella et al. 2009). The fraction of rotationally supported early-type galaxies is about 60% and it does not change significantly between $z \sim 1$ and $z \sim 0$ (van der Wel & van der Marel 2008). There are also systematic differences in the interstellar medium content. In the Local Universe, where H I systematic measurements are available, only a handful of elliptical galaxies have H I detected in them, compared with the plethora of spirals and irregulars, reflecting the much smaller $\mathrm{H\,I}/M_*$ ratios in ellipticals compared with later-type galaxies (e.g., Haynes & Giovanelli 1984; Noordermeer et al. 2005).

It has been known for many years that the observed mix of different morphological classes at the present epoch also depends on the galaxy environment. Early-type morphologies are preferentially found in dense, cluster-like regions. This idea can be traced back to Hubble, but the major impact on the astronomical community started after Dressler's study of 55 nearby galaxy clusters (Dressler 1980). The existence of the morphology–density relation is presumably linked to the physical processes that govern the star formation (and morphological transformation) of galaxies and the connection of these to the environments of individual galaxies.

After the morphology–density relation in clusters was established (e.g., Dressler 1980), the existence of the relation was extended to the group environments (e.g., Postman & Geller 1984) at low redshift. Later, the evolution with redshift was measured (e.g., Dressler et al. 1997; Postman et al. 2005; Fasano et al. 2000; Desai et al. 2007). There is evidence that the evolution in intermediate-density environments has occurred more recently than in high-density environments (Smith et al. 2005). Also, it appears that the morphological mix of early-type clusters has changed with time (Fasano et al. 2000; Postman et al. 2005). Ultimately, understanding the origin of the morphology–density relation can help to disentangle the relative roles of nature (conditions at epoch of galaxy formation) and nurture (environment-dependent processes) in determining the properties of galaxies.

It is known that galactic mass also plays a major role in determining the properties of galaxies, since both color-specific star formation rates and morphologies are strongly correlated with the stellar mass of galaxies (e.g., Kauffmann et al. 2003). The recent evidence that the stellar mass function of galaxies itself depends on the environment (Baldry et al. 2006; Bolzonella et al. 2009) complicates the separation of the relative roles of mass (which could be regarded as "nature") and of environment ("nurture"). This linkage also complicates the interpretation of environmental effects in any sample of galaxies that contains a significant range of masses, since different environments within such a sample will contain a different mix of masses. This in turn can easily produce the appearance of a "spurious" environmental dependence through the dependence of will contain galaxy properties on mass (see Tasca et al. 2009 and Cucciati et al. 2010).

Several physical processes have been suggested which could enhance the transformation of late-type to early-type galaxies (and star-forming ones to quiescent ones) in dense regions (see Boselli & Gavazzi 2006 for recent review of these processes). Mergers and interactions with other galaxies or with the cluster potential (e.g., Toomre & Toomre 1972; Barnes 1988) are purely gravitational processes. Galaxy harassment combines the cumulative effect of the interaction of a galaxy with close neighbors with the interaction of the total cluster potential (Moore et al. 1998). Ram pressure stripping may be responsible for the removal of cold gas when a galaxy infalls with high velocity into a dense medium (Gunn & Gott 1972; Quilis et al. 2000). While ram pressure stripping is expected to be most effective in the dense intracluster medium, Rasmussen et al. (2006) have shown that gas stripping by the intragroup medium may also be rapid enough to transform late-type galaxies to S0s over a few Gyr. Strangulation (or starvation) is a process that may remove a halo of hot diffuse gas after a galaxy becomes a satellite in a larger dark matter halo (Larson et al. 1980; Balogh & Morris 2000). Bamford et al. (2009) placed these processes in two broad categories: (1) those processes that will quench star formation and act on morphology passively, through the fading of spiral arms and reduction of the prominence of the disk after star formation has stopped (e.g., strangulation) and (2) those processes that will directly affect the stellar kinematics and galactic structure and also lead to a cessation of star formation (e.g., mergers). While both categories can produce S0s, only the second one can produce true elliptical galaxies.

One way to assess the relevance of a type-transformation process is to constrain its timescale. However, there are a number of timescales related to a given process, and the interpretation of an observed transformation rate is not necessarily unique. Here we differentiate between the following timescales. The "physical timescale" t_p is a measure for a duration of the transformation of an individual galaxy. For example, the t_p of the morphological transformation would be the average time that has elapsed since the beginning of the morphological transformation, when a galaxy would still be classified as late, till the point in its evolution when it will be classified as early. Sometimes it is more relevant to express the transformation in a probabilistic sense, as in radioactive decay. We can then quantify how long it will take (on average) for a galaxy of a given class to transform to a galaxy of some other class. This is a "statistical timescale" t_s, which is just the inverse of the average transformation rate. Finally, there is an observed "rate timescale" t_η (obtained as the inverse of the observed rate), based on the real observations, whose meaning depends on its relation to the other timescales. If $t_p \ll t_\eta$, then t_η will be of order t_s. However, if t_p is of order t_η then t_η will be more a measure of t_p. The interpretation of the observed t_η therefore depends on the physical timescale t_p.

In this paper, the main aim is to study the changes in the morphological mix of galaxies in group environments that have occurred in the time interval between $z \sim 1$ down to $z \sim 0.1$. Our primary goal is to understand the role of the group environment in the transformation of galaxies over this redshift range. We carry out the analysis by measuring the redshift evolution of the fraction of galaxies with early-type morphologies in the total population of galaxies of a given luminosity or stellar mass in three different environmental samples: group, field, and isolated galaxies. This leads us to construct the morphological transformation rate, normalized to the number of galaxies in the "pre-transformation" state (i.e., late morphological type) in different environments and quantify the timescales of the morphological transformation in

different environments. We then compare these rates with the equivalent ones defined by overall color and by star formation rate indicators that reflect the quenching of star formation activity. Determination of the transformation rates, i.e., of the flux of galaxies crossing through a chosen dividing line, should be less sensitive to the exact values chosen to divide galaxies into different classes than, for example, the quantity that directly reflects the partitioning of galaxies into these classes (such as crossing or transition mass defined as the mass at which two classes are equally partitioned).

The analysis is based on the COSMOS field (Scoville et al. 2007a), relying heavily on the zCOSMOS data (Lilly et al. 2007, 2009) necessary for the precise, small-scale definition of environment on a group scale. This paper is closely related to the number of other studies based on the data in the COSMOS field that have been aimed to address the complex interplay between galaxy properties and environment up to $z \sim 1$–1.5. A complementary analysis exploring galaxy colors in the group catalog of Knobel et al. (2009) is presented in Iovino et al. (2010). Scoville et al. (2007b), Capak et al. (2007a), Guzzo et al. (2007), Cassata et al. (2007), and Ideue et al. (2009) study the galaxy property–environment relation using data sets based on photometric redshifts. Tasca et al. (2009), Cucciati et al. (2010), and Bolzonella et al. (2009) extend this study by using high precision spectroscopic redshifts and the continuous density field of Kovač et al. (2010). Moreover, the environmental dependence of specific galaxy populations has been addressed in separate studies, e.g., infrared-luminous galaxies in Caputi et al. (2009), active galactic nuclei (AGNs) in Silverman et al. (2009) and post-starburst galaxies in Vergani et al. (2010). The relation between the galaxy distribution and that of the underlying matter density field is explored in Kovač et al. (2009).

Throughout the paper we use a concordance cosmology with $\Omega_m = 0.25$, $\Omega_\Lambda = 0.75$, and $H_0 = 70$ km s^{-1} Mpc^{-1}. Magnitudes are given in the AB system.

2. THE zCOSMOS SURVEY

2.1. Details of the Survey

COSMOS (Scoville et al. 2007a) is a multi-wavelength survey of a 2 deg^2 equatorial field, observed so far by the major earth- and space-based facilities, e.g., the *Hubble Space Telescope* (*HST*), *Spitzer*, the *Galaxy Evolution Explorer* (*GALEX*), *Chandra*, Subaru. zCOSMOS (Lilly et al. 2007) is a spectroscopic redshift survey in this field carried out with the VIMOS spectrograph on the ESO UT3 8-m VLT. The zCOSMOS-bright part of the survey is flux limited at $I_{\rm AB} < 22.5$, and will ultimately obtain over 20,000 spectra. At this flux limit, the redshifts of the majority of the observed galaxies fall in the range $0 < z < 1.4$. A higher redshift range, $1.4 < z < 3$ is targeted in the zCOSMOS-deep program. Here, we use the first 10,000 spectra from zCOSMOS-bright, which we refer to as the "10k sample" (Lilly et al. 2009). The high-quality photometry in the COSMOS field also allows us to derive accurate photometric redshifts, with an uncertainty of $0.023(1 + z)$ or better. These are used to understand the spectroscopic completeness of the survey (see Lilly et al. 2009).

The rest-frame absolute magnitudes of all $I_{\rm AB} < 22.5$ targets are measured using the spectral energy distribution (SED) fitting employing the ZEBRA code (Feldmann et al. 2006). The magnitudes are obtained as the best fit normalized to each galaxy photometry (Capak et al. 2007b) at the best available redshift, spectroscopic or photometric (P. Oesch et al. 2010, in preparation, see also Zucca et al. 2009). Stellar masses M_* are obtained from fitting stellar population synthesis models to the SED of the observed magnitudes as described in Bolzonella et al. (2009) and Pozzetti et al. (2009), using the best available redshift. The stellar masses that we use are obtained with the Bruzual & Charlot (2003) libraries and the Chabrier initial mass function (Chabrier 2003), the Calzetti et al. (2000) extinction law with $0 < A_V < 3$, and solar metallicities. The assumed star formation history (SFH) is decreasing exponentially with a timescale τ, taking values from the interval $0.1 < \tau < 30$ Gyr. The stellar mass is obtained by integrating the SFH over the galaxy age, from which the mass of gas processed by stars and returned to the interstellar medium during their evolution ("return fraction") has been subtracted. See Bolzonella et al. (2009) for more details.

2.2. The zCOSMOS 10k Group Catalog

The detailed description of our group-finding algorithm and the group catalog are presented in Knobel et al. (2009). Here, we outline only the most important points regarding the group catalog.

Knobel et al. (2009) combine two standard group searching algorithms: friends-of-friends (FoF) and the Voronoi–Delaunay method (VDM) to define groups in the 10k zCOSMOS. The group-finding parameters are optimized based on tests of the COSMOS mock catalogs (Kitzbichler & White 2007) designed to match the geometrical and sampling properties of the 10k zCOSMOS catalog. Knobel et al. (2009) also developed a new "multi-pass" strategy that optimizes group finding over a range of richnesses by first optimizing for the largest groups and then subsequently moving down to groups with a smaller number of observed members.

The group catalog that we use in this work is the so-called "one-way-matched" catalog, which is the intersection of the independently created FoF and VDM catalogs. In total, there are 800 groups with at least two members in the current 10k sample. Over 100 of these groups have at least 5 spectroscopically observed members.

Extensive comparisons with the mock catalogs (Kitzbichler & White 2007) have established that the zCOSMOS 10k group catalog has a relatively high purity and completeness—82% and 81%, respectively, for groups with $N \geqslant 5$, and only marginally lower for the poorer groups. It should, however, be appreciated that these numbers are based on comparisons with the ideal group catalogs that could have been constructed (with two or more spectroscopic members per group) from a sparsely sampled "10k-like" dataset, rather than the actual set of all groups in the COSMOS volume. As a result, some of the galaxies that are not currently placed in a group are nevertheless likely to be in a group which will be identified in the future with higher sampling of the full survey. The current "non-group" sample will therefore contain some "group" galaxies, and this contamination will act to reduce observed differences between group and non-group populations. Partly for this reason, as discussed below, we will usually use the entire galaxy population that we have observed spectroscopically, selected without regard to environment, as our control sample. This also reflects the traditional definition of a "field sample."

Due to the non-uniform sampling scheme of the current 10k zCOSMOS survey (Lilly et al. 2007, 2009), the fraction of group members observed (as well as the chance of recognizing the poorer groups) will be a function of positions on the sky. We therefore correct the observed number of members for

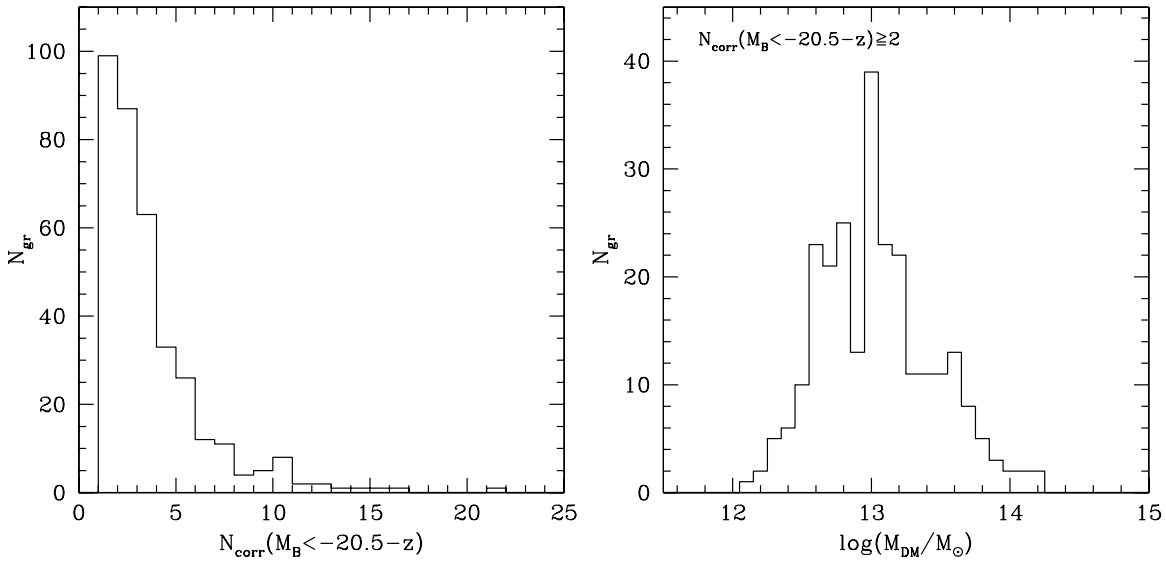

Figure 1. Properties of the zCOSMOS groups ($0.1 < z < 1$) used for the current analysis. Left: distribution of the "corrected richness," i.e., the number of members corrected for sampling incompleteness, above $M_B < -20.5 - z$. Right: distribution of the estimated halo masses for the zCOSMOS groups shown in the left. The halo masses are estimated by comparison with the COSMOS mock catalogs of Kitzbichler & White (2007). The majority of the groups have less than 10 corrected $M_B < -20.5 - z$ members and masses in the range $12 < \log(M_{DM}/M_\odot) < 14$, emphasizing that the sample involves cosmic structures well below the masses of rich clusters of galaxies.

each group by the overall sampling fraction of the survey at that location, taking into account both the spatially variable spectroscopic sampling rate and the redshift-dependent success rate in yielding a high confidence redshift (using the corrections derived in Knobel et al. 2009, Equation (23)). We will refer to this as the corrected richness. Using the mock catalogs, Knobel et al. (2009) find that the corrected richness shows a relatively tight correlation with the estimated halo mass (see Figure 13 in Knobel et al. 2009) starting from groups with only two spectroscopically confirmed members. However, it should be noted that such defined corrected richness of the group overestimates the true number of group members by about 50%–100% on average (when using the $M_B < -20 - z$ members), depending on the number of observed members (Knobel et al. 2009). Therefore, the corrected richness of a group should not be interpreted as a true number of members, but instead, it should be understood as an overall property of a group of any size, well correlated with its halo mass.

For any given physical group, this corrected richness will vary with redshift due to the changing luminosity limit that is associated with the observed *I*-band limit. We can deal with this by considering groups with a given corrected richness above some fixed luminosity limit, allowing this limit to evolve with redshift to account for the luminosity evolution of individual galaxies as best we can. We refer to such a set of groups as a "volume-limited" sample in that it should contain all groups of a given type, but this sample could still be potentially affected by the so-called progenitor bias since infall of new members will produce new groups in this volume-limited sample at later epochs. Moreover, given that the original group catalog is generated from a flux limited sample, there will be a slight bias with redshift because poor groups are more difficult to detect at high z than at low z. However, the distribution of corrected richness with redshift is rather flat, reassuring us that this effect is minor.

The distribution of corrected richnesses using the luminosity limit $M_B < -20.5 - z$ in $0.1 < z < 1$ is shown in the left panel in Figure 1. The corrected richness for the majority of the 10k zCOSMOS groups was measured using the members above $M_B < -20.5 - z$ less than 10.

For groups with $N \geqslant 5$, Knobel et al. (2009) provide the measure of the observed velocity dispersion. Moreover, Knobel et al. (2009) also give an estimate of the virial mass of the dark matter (DM) halo for all of the groups by assigning a halo mass to each group using the empirical relation between the halo mass and the corrected observed richness, calibrated at each redshift on the mock catalogs (Kitzbichler & White 2007). The distribution of these estimated halo masses for the zCOSMOS groups with corrected richness of at least two members with $M_B < -20.5 - z$ detected in $0.1 < z < 1$ is shown in the right panel in Figure 1. The redshift distribution of the DM halo masses is also rather flat. The groups which we are using for the analysis typically have halo masses in the range $12 < \log(M_{\rm DM}/M_\odot) < 14$. This emphasizes that the zCOSMOS volume to $z \sim 1$ does not contain rich clusters of galaxies.

2.3. Isolated Galaxies

In parallel, we measure the morphological mix of galaxies in a sample of isolated galaxies, to further highlight the possible environmental segregation of galaxy morphological types. For this purpose, we use the sample of isolated galaxies defined by Iovino et al. (2010) as follows. First, the Voronoi volume is estimated for each galaxy in the zCOSMOS flux limited $I_{\rm AB} < 22.5$ sample in the area defined by $149.^\circ57 <$ R.A. $< 150.^\circ41$ and $1.^\circ76 <$ decl. $< 2.^\circ68$ in $0.1 < z < 1$. These Voronoi volumes are normalized by the median Voronoi volume in $\Delta z = 0.2$ centered at each galaxy redshift, to correct for the changing mean intergalaxy separation with redshift. Galaxies with the normalized Voronoi volume within the highest quartile of these volumes are defined as the isolated galaxies. Moreover, galaxies with Voronoi volumes that are too large determined with respect to the normalized mean Voronoi volume ($\sim$10% of the preliminary sample of isolated galaxies), most probably affected by the survey borders, and galaxies determined to be in

groups (∼14% of the preliminary sample of isolated galaxies) are removed from the sample. Based on the $I_{AB} < 22.5$ mock catalogs, about 90% of the galaxies defined as isolated using the described procedure should be the single occupants of their halos.

2.4. Field Galaxies

Following an original practice, in this paper we refer to a "field" sample as being all galaxies selected without regard of environment. In comparisons of the various relations, the field sample will always be chosen to exactly match the selection of the group and isolated samples of galaxies with regard to all non-environmental parameters, e.g., luminosity, mass, type, redshift.

2.5. Morphologies

The COSMOS field is the largest contiguous field covered by *HST* Advanced Camera for Surveys (ACS) images. The *HST* observations (Koekemoer et al. 2007) were taken in the F814W filter. ACS imaging affords the possibility to derive robust structural parameters and to confidently morphologically classify all galaxies into "Hubble types" down to about 24 mag (and possibly deeper), well below the flux limit of zCOSMOS-bright.

Here we use the structural parameters and morphological classification based on the Zurich Estimator of Structural Types (ZEST) and presented in Scarlata et al. (2007). The ZEST classification scheme is based on a principal component analysis of five non-parametric diagnostics of galaxy structure: asymmetry A, concentration C, Gini coefficient G, the second-order moment of the brightest 20% of galaxy pixels M_{20}, and the ellipticity ϵ. The morphological classification is performed in the space of the first three eigenvectors, which contain most of the variance of the original non-parametric quantities. At each point in the three-dimensional eigenvector space, a morphological class is assigned based on inspection with the naked eye and the median Sérsic index of all the galaxies in that cell.

Galaxies are classified by ZEST into elliptical, disk, and irregular galaxies. The disk galaxies are further split in four bins, namely bulgeless, small-bulge, intermediate-bulge, and bulge-dominated disk galaxies.

In the following we consider all galaxies that are classified by ZEST as either "elliptical" or "bulge-dominated" systems, i.e., specifically ZEST Classes 1 and 2.0, as "early-type". All other ZEST types are collectively considered to be "late-type" galaxies. In terms of the conventional Hubble classification scheme, our division would probably be between Sa and Sb.

3. SAMPLE DEFINITION

While there are about 40,000 galaxies in the zCOSMOS field which satisfy the survey selection criteria $I_{AB} < 22.5$ mag (the "40k sample" catalog), at the current stage of the project only about 10,000 spectra (10k sample catalog) have been obtained. In this sample every redshift has been assigned a quality flag based on the confidence of the measured spectroscopic redshift. This quality flag is calibrated using both the repeatability of the spectroscopic measurement and the consistency of the photometric redshift estimates (see Lilly et al. 2007, 2009 for more details). In this paper, we use all galaxies with spectroscopic confidence class 3 and 4 and all galaxies with a lower spectroscopic confidence class but whose spectroscopic redshift is consistent with their rather accurate photometric redshift. The sample consists of 8478 galaxies, representing overall 88% of the 10k zCOSMOS-bright sample at $z < 1.2$, increasing to 95% for the $0.5 < z < 0.8$ subsample, with an overall redshift reliability of 98.6%. We refer to this sample as the high confidence class 10k sample (HCC 10k).

Due to the inhomogeneous sampling of galaxies with spectroscopic redshifts, we limit our analysis to the zCOSMOS region defined by $149.^{\circ}55 \leqslant$ R.A. $\leqslant 150.^{\circ}42$ and $1.^{\circ}75 \leqslant$ decl. $\leqslant 2.^{\circ}70$, in which the sampling is both higher and more homogeneous. The area is slightly smaller for the isolated galaxies (see Section 2.3). This is the same region as used by Iovino et al. (2010) for a parallel analysis investigating the color segregation of galaxies in groups (e.g., see Figure 1 in Iovino et al. 2010).

3.1. Correction for the Spectroscopic Incompleteness

In zCOSMOS, the targets to be observed spectroscopically are selected independently of the galaxy properties, except for the requirement of $15.0 < I_{AB} < 22.5$. The failure to assign a redshift to observed spectra may have several causes, some of which may depend directly or indirectly on the properties of the target galaxies. We therefore adopt a weighting scheme to correct for the objects observed spectroscopically which have insufficiently good redshifts to be included in the HCC 10k sample (including complete failures) taking into account only galaxy properties. We define a multidimensional space by the selection magnitude I_{AB}, the rest-frame $(U - V)_0$ color, morphological type, and redshift, relying on the values calculated using high quality photometric redshifts. For each galaxy, the multi-parameter space is sampled for galaxies of the same morphological class within an interval, centered on the galaxy in question, that is 0.25 mag in I_{AB} magnitude, 0.25 mag in the rest-frame $(U - V)_0$ color, and 0.1 in redshift. We then define the inverse weight w_i of each galaxy i in the HCC 10k sample as the fraction:

$$w_i = \frac{N^i_{\rm HCC10k}}{N^i_{\rm 10k}}, \quad (1)$$

where $N^i_{\rm HCC10k}$ is the number of galaxies in the HCC 10k sample and $N^i_{\rm 10k}$ is the number of galaxies in the total 10k sample which are neighbors of the ith galaxy in the above defined manner in the multidimensional $I_{AB} - (U - V)_0 - z_{\rm phot}$-morphology space. In those cases where a galaxy in the 10k sample could not be assigned any of the properties considered (I_{AB}, $(U - V)_0$, $z_{\rm phot}$ and morphology) the galaxy is excluded from the analysis. We can neglect these galaxies given that their exclusion is based on the absence of data and not directly on the properties of galaxies. Moreover, they constitute a negligible fraction (<4%) of the total sample. The final number of the group, field, and isolated galaxies is 1859, 5671, and 1147 in $0.1 < z < 1$ and in the selected area (see above), respectively.

3.2. Computing the Fraction of Galaxies and Errors

Having defined the inverse weights of the galaxies in the HCC 10k sample using Equation (1), the fraction of galaxies of a given morphological type within any given galaxy sample is straightforwardly computed from the HCC sample in terms of the sum of these individual weights. Specifically, the total number of galaxies of a given morphological type T (using the ZEST morphological classification) in a given sample of

Table 1
Number of (Non-weighted) Galaxies in the Luminosity-complete Samples

$M_{B,\mathrm{compl}}$ Limit z Range	$M_B < -19 - z$ $0.1 < z < 0.5$	$M_B < -19.5 - z$ $0.1 < z < 0.7$	$M_B < -20 - z$ $0.1 < z < 0.9$	$M_B < -20.5 - z$ $0.1 < z < 1$
Group($M_B < M_{B,\mathrm{compl}}$)	564	665	605	329
Group($M_B < 20.5 - z$)	275	321	386	329
Field	1391	1924	2098	1319
Isolated	240	334	340	206

galaxies is calculated using

$$N_T^K = \Sigma_k \frac{1}{w_k(T)}, \quad (2)$$

and summing over all T type galaxies in the K-subsample of the HCC 10k sample. Similarly, the total (weighted) number of galaxies of any type can be calculated using

$$N_{\mathrm{ALL}}^K = \Sigma_k \frac{1}{w_k} \quad (3)$$

summing over all galaxies in the K-subsample of the HCC 10k sample. The fraction of galaxies of a given morphological type T is then straightforwardly given by

$$f_T^K = \frac{N_T^K}{N_{\mathrm{ALL}}^K}. \quad (4)$$

The index K refers to the sample in which the morphological fraction of galaxies is calculated and is defined by environment, as well as by luminosity or stellar mass. In considering sets of galaxies defined by luminosity or mass, we decided to only consider intervals in either quantity which is essentially complete over a given redshift range, i.e., not to attempt a V/V_{max} type correction for incompleteness.

Uncertainties in the observed fractions are estimated using a bootstrap resampling of the given subsample of galaxies, setting the error bars in the f_T^K as the standard deviation in the distribution of fractions resulting from 1000 Monte Carlo bootstrap realizations.

4. RESULTS

In this section, we measure and compare the morphological mix of galaxies residing in different environments (groups, isolated, and field) lying within the zCOSMOS volume in the redshift interval $0.1 < z < 1$. As noted above, we refer to the morphological types 1 and 2.0 together as the "early-type" galaxies and the remainder as "late-type."

Given that the zCOSMOS groups contain typically only a few members, we cannot measure a meaningful morphological fraction of galaxies in individual groups, as is common when studying similar relations in rich clusters of galaxies, but rather combine all galaxies residing in groups with similar properties to build a statistically meaningful sample of galaxies. It will become clear that, even with this large set of high-redshift groups, the selection of subsamples of groups and galaxies for study is primarily guided by the need to have statistically usable numbers of galaxies in each of the bins.

Furthermore, the current sparse sampling of zCOSMOS means that we cannot meaningfully distinguish between central and satellite galaxies within the groups.

Much recent work aimed to address the redshift evolution of a morphological mix of galaxies targeted rich clusters individually which could be easily identified at high z (see recent work by Desai et al. 2007 and references therein). For the precise reconstruction of the groups one needs high resolution spectroscopic redshifts in a relatively large continuous volume. Needless to say, the additional requirement is high resolution imaging over the full survey area in order to reliably measure galaxy morphologies. The zCOSMOS groups are identified in a larger volume than in the two previous high-redshift ($z \sim 1$) spectroscopic surveys, VVDS (Le Fèvre et al. 2005) and DEEP2 (Davis et al. 2003). Moreover, only color properties of galaxies in group environments have been studied in $0.25 < z < 1.2$ (Cucciati et al. 2009) and in $0.75 < z < 1.3$ (Gerke et al. 2007) in the VVDS and DEEP2, respectively.

4.1. Morphological Fraction of Galaxies in the Luminosity-complete Samples

To study the dependence of morphological segregation of galaxies in groups on the luminosity of galaxies, it is useful to first define "luminosity-complete," i.e., "volume-limited," samples of galaxies. We do this primarily to compare with the results in the literature, before turning to mass-selected samples below.

We define four galaxy samples which satisfy the following criteria: $M_B < -19 - z$ at $0.1 < z < 0.5$, $M_B < -19.5 - z$ at $0.1 < z < 0.7$, $M_B < -20 - z$ at $0.1 < z < 0.9$, and $M_B < -20.5 - z$ at $0.1 < z < 1$. We chose to use the (rest-frame) M_B magnitude because it is well matched to the observed I-band selection of zCOSMOS-bright at high redshifts, with an exact match at $z \sim 0.8$, thereby assuring that the completeness of the zCOSMOS galaxies is not color dependent (see Iovino et al. 2010). At best, the "$-z$" term approximately accounts for the luminosity evolution of individual galaxies $\Delta M_B = -1 \times \Delta z$ (see Kovač et al. 2010 for discussion). The number of galaxies in the luminosity-complete samples is given in Table 1. As shown in Figure 2, these galaxy samples should be statistically complete.

Correspondingly, for each of these luminosity-complete galaxy samples, we can also define a set of "luminosity-complete" groups that satisfy the group criteria, i.e., that their corrected richness is at least two above these same galaxy luminosity limits. These groups should also be "volume-limited" in a sense, although it is clear that the accretion of new members may lead to a change in the group population through the relevant redshift range.

For the sample of volume-limited groups it is true that some groups will contain only one galaxy with spectroscopic redshift above the adopted luminosity limit, but one needs to note that all of these groups have at least two spectroscopically confirmed members, and therefore they are all real entities (obviously, within the uncertainties of the group finding process). The reason for the use of all the groups with corrected richness of at least two without respect to the number of spectroscopically confirmed members above the given luminosity limit is in order

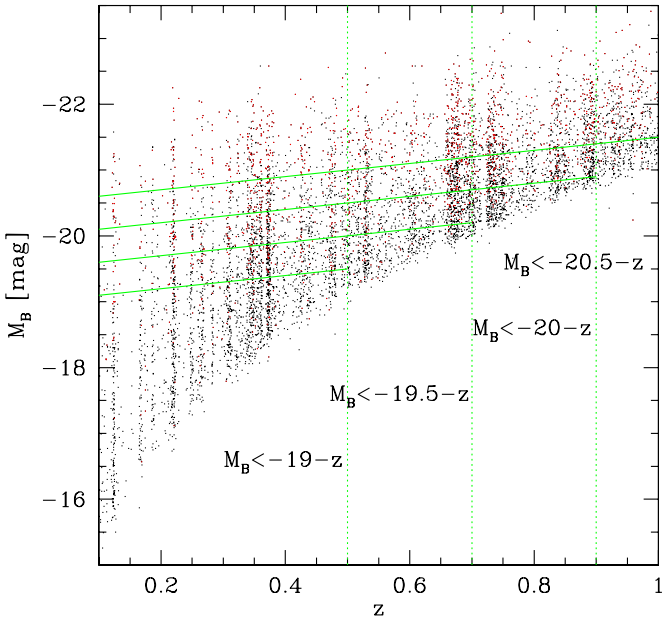

Figure 2. Rest-frame *B*-band magnitude as a function of redshift for the 10k zCOSMOS sample. Galaxies of early morphological type (ZEST types 1 and 2.0) are colored red. The green lines define the four luminosity-complete samples used in the analysis.

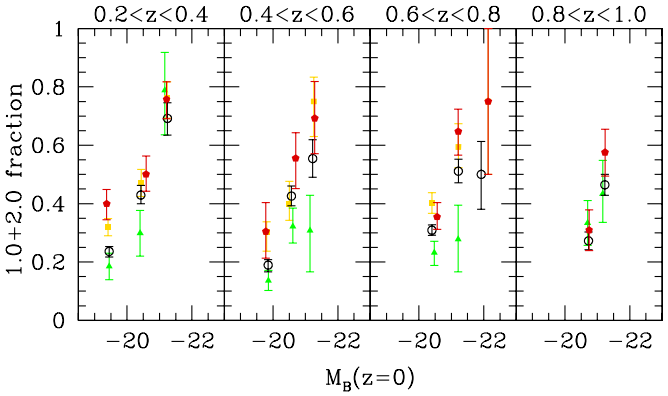

Figure 3. Fraction of early-type galaxies at a given M_B magnitude, evolving the luminosity to $z = 0$. The red pentagons and yellow squares represent the group galaxies, the empty black circles represent the field galaxies and the solid green triangles represent the isolated galaxies. The group galaxies are included in the analysis only if the group has a corrected richness of at least two in the given luminosity-complete sample (yellow squares) or if the group has the corrected richness of at least two in the $M_B < -20.5 - z$ sample (red pentagons, which are therefore complete across all panels). The fraction of galaxies in the different panels are calculated using only those galaxies from luminosity-complete samples in the narrow redshift slices (indicated at the top of each panel). The fraction of early-type galaxies is higher for brighter galaxies in all redshift bins. The fractions of early-type galaxies at fixed M_B are also higher for galaxies residing in groups compared with the overall population of field galaxies. The fractions of isolated galaxies with early-type morphologies tend to be the lowest.

to keep the number of galaxies statistically meaningful when split to bins in redshift, luminosity (or mass), and environment, and when using the unique evolving luminosity limit over the whole redshift range. We have carried out tests which assure us that the obtained results are not driven by how we select volume-limited samples—i.e., with the two corrected or with the two spectroscopically confirmed members above the given luminosity limit.

With these considerations and caveats in mind, Figure 3 shows the fraction of early-type galaxies in different environments as a function of (evolving) absolute M_B magnitude. The black points show the field sample (all galaxies) while the green points show the set of isolated galaxies. The yellow points in each panel show the subset of galaxies that appear in the corresponding complete set of groups at that redshift, i.e., with more than two corrected members above a luminosity threshold for which we are complete, i.e., $M_B < -19 - z$ for the $0.2 < z < 0.4$ panel, $M_B < -19.5 - z$ for the $0.4 < z < 0.6$ panel, $M_B < -20 - z$ for the $0.6 < z < 0.8$ panel. The red points represent galaxies in groups with two or more members above $M_B < -20.5 - z$, for which we are complete across the whole redshift range. Apart from the caveats above about infall and progenitor bias, the group galaxies that are represented by the red points should therefore be directly comparable across the whole redshift range.

It is clear from Figure 3 that the fraction of early-type galaxies is higher for brighter galaxies in all redshift bins, covering the range from $z = 0.1$ to $z = 1$. This reflects the strong and well-known dependence of morphology on mass or luminosity. In addition, however, the fraction of early-type galaxies at fixed M_B is higher for galaxies residing in groups compared with the overall population of field galaxies. This holds for every luminosity sample and at every redshift bin considered, even though the difference is sometimes within the margin of error. Similarly, the fractions of isolated galaxies with early-type morphologies tend to be lower than in the sample as a whole. In the highest redshift bin ($0.8 < z < 1$), the differentiation of the early-type fraction of galaxies in the different environments becomes negligible. Here, the morphological mix of early-type galaxies is within the errors the same in all environments.

Comparing the panels across the diagram, it is clear that the fraction of early-type galaxies at a given luminosity increases with time. This is more clearly seen in Figure 4, which shows the redshift/look-back time evolution of the fraction of early-type galaxies in three narrow ranges of M_B which are explored over three redshift intervals: $0.1 < z < 0.5$, $0.1 < z < 0.9$, and $0.2 < z < 1$. As in Figure 3, the red points represent the members of a set of groups that is, in principle, volume limited up to $z = 1$, whereas the yellow points represent the members of a set of groups that is only volume limited within each individual panel. The redshift evolution of the early-type fraction seen in Figure 4 indicates a clear build-up over time of the population of luminous early-type galaxies in the group and field environments. For the isolated galaxies the build-up of early-type galaxies is detected only for the faintest galaxies. For the isolated galaxies with $-21 - z < M_B < -20 - z$ the fraction of early types stays more or less constant since $z = 0.9$, but the error on the measured fraction at the lowest redshift is rather large and we do not have a sufficient number of isolated galaxies with $-22 - z < M_B < -21 - z$ to reliably carry out this analysis.

From Figure 3, it can be seen that the fraction of early-type galaxies in the group environment is higher than the fraction of early-type galaxies in the field (all galaxies), which is again higher than the early-type fraction in the isolated galaxies. By fitting a simple linear relation between the fraction of early-type galaxies and the look-back time, the data suggest that the morphological transformation of galaxies from late to early type has generally happened earlier for galaxies residing in groups than for galaxies of the same luminosity in the field, coupled with an overall trend for the transformation to occur earlier for more luminous galaxies. We will quantify this further below.

The evolution of the early-type fraction over cosmic time and its dependence on luminosity qualitatively mirrors (i.e., it is

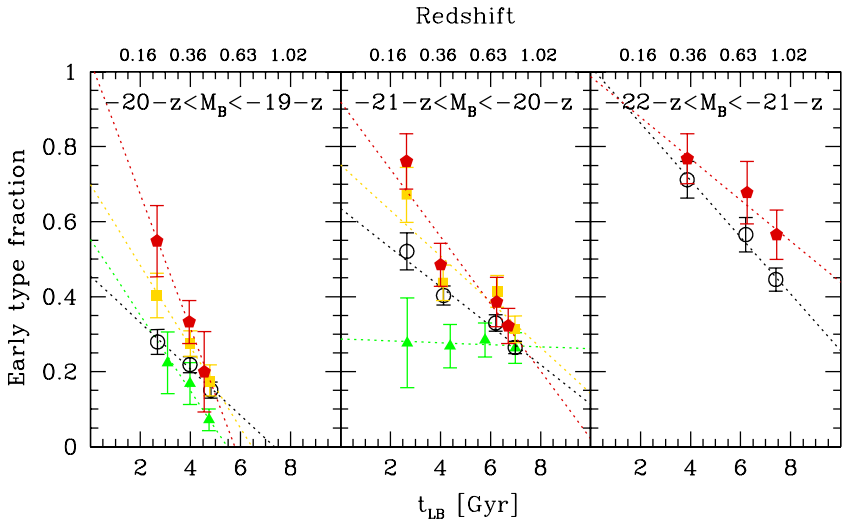

Figure 4. Redshift/look-back time evolution of the fraction of early-type galaxies of a given luminosity in different environments. As in Figure 3, the red pentagons and the yellow squares represent the group galaxies, the black circles represent the field galaxies, and the green triangles represent the isolated galaxies in the indicated M_B-bins of galaxies. We consider the two following types of groups for this analysis: with a corrected richness of at least two in the $M_B < -19-z$ (yellow squares left panel), in the $M_B < -20-z$ (yellow squares middle panel) or in the $M_B < -20.5-z$ sample of galaxies (red pentagons, therefore complete across all panels). For the analysis, we consider only redshift intervals in which galaxies of a given luminosity are drawn from the luminosity-complete samples: $0.1 < z < 0.5$, $0.1 < z < 0.9$, and $0.2 < z < 1$ from left to right, respectively. The symbols are plotted along the horizontal axis at the median look-back time/redshift of galaxies in the considered bin. The dotted lines are the linear fits to the $f_{\rm early}$–$t_{\rm LB}$ relation for the various samples, marked in the same color as the corresponding early-type fractions. The results indicate a build-up over time of the population of early-type galaxies in both the group environment and the field environment (all galaxies) and, especially at fainter M_B, also in the isolated sample.

(A color version of this figure is available in the online journal.)

inverse to) the evolution and its environmental and luminosity dependences of the fraction of blue galaxies in the zCOSMOS group, field and isolated samples, investigated by Iovino et al. (2010).

4.1.1. Comparison with Literature

An exact comparison of our results with the previously published studies of the morphological mix of galaxies in $0.1 < z < 1$ is hindered by the different morphological classifications, and further complicated by the different selection of galaxies and the generally much denser environments. However, we can qualitatively place our results within the previous results obtained with the luminosity-complete samples.

Galaxies which reside in the zCOSMOS groups reside also in the regions of the highest density in the continuously defined zCOSMOS density field (Kovač et al. 2010). The higher fractions of the early-type galaxies in the groups relative to the field and isolated (when measured) samples are consistent with the morphology–density relations obtained in the COSMOS field (Tasca et al. 2009; Capak et al. 2007a; Guzzo et al. 2007; Cassata et al. 2007) at similar luminosity limits and similar investigated environments.

The ZENS project (C. M. Carollo et al. 2010, in preparation) is a *B* and *I* wide-field imaging survey of galaxies in a statistically and luminosity-complete sample of 185 groups at $z \sim 0.05$ extracted from the 2PIGG catalog (Eke et al. 2004) with more than five cataloged galaxy members, in order to measure morphologies and quantify substructure (e.g., bars, bulges, and disks), and to determine the presence and properties of faint structures. The observed increase of the fraction of early-type galaxies with luminosity in the group environment is clearly detected in the $z \sim 0.05$ ZENS groups down to $M_B = -17$ (A. Cibinel et al. 2010, in preparation). Going to higher redshift, Wilman et al. (2009) measured the morphological mix of $M_r < -19$ galaxies in the group and non-group environments using a sample of optically selected groups in $0.3 \leqslant z \leqslant 0.55$ from the Canadian Network for Observational Cosmology redshift survey (Carlberg et al. 2001; Wilman et al. 2005). They conclude that the fraction of S0 galaxies in groups at $z \sim 0.4$ is as at least as high as in clusters and X-ray-selected groups, and it is higher than the fraction of S0s of the sample of galaxies not classified to belong to a group. The fraction of elliptical galaxies at fixed luminosity does not appear to be significantly different in the group and non-group environment. Taking the fractions of S0s and ellipticals together, the results of Wilman et al. (2009) and our results at $z \sim 0.4$ are in qualitative agreement, in the sense that at this redshift we measure a higher fraction of early-type galaxies in the groups than in the field or isolated (i.e., non-group) sample of galaxies at all luminosities.

Desai et al. (2007) combined the data from the various studies of the morphological content in clusters in order to construct the redshift evolution of the morphological mix of galaxies. Using the fractions of early-type galaxies (ellipticals and S0s) measured in 10 ESO Distant Cluster Survey (EDisCS; White et al. 2005) clusters in $0.5 < z < 0.8$ (Desai et al. 2007) and the literature data compiled by Fasano et al. (2000), both down to $M_V = -20$ (using cosmology with $\Omega_m = 1$ and $H_0 = 50$ km s^{-1} Mpc^{-1}), Desai et al. (2007) conclude that the fraction of S0 galaxies in clusters increases about twofold from $z = 0.4$ to $z = 0$, while the fraction of ellipticals stays constant over the same redshift interval. The EDisCS results ($M_V < -20$) combined with the equivalent studies of seven clusters from Postman et al. (2005) at $0.8 < z < 1.27$ ($M_V < -19.27 - 0.8z$) are consistent with no evolution in the morphological mix in clusters over the entire $0.4 < z < 1.25$ interval (using $\Omega_m = 0.3$, $\Omega_\Lambda = 0.7$, and $H_0 = 70$ km s^{-1} Mpc^{-1}, Desai et al. 2007), suggesting that $z \sim 0.4$ is an epoch at which the S0 fraction in cluster cores begins to grow. However, our results are consistent with the constant build-up of early types since $z = 1$ or $z = 0.9$ in at least group and field environments for $-22 - z < M_B < -21 - z$ or $-21 - z < M_B < -20 - z$

galaxies, respectively. Ignoring the differences in the luminosity selection (the median $B-V$ color of the field $M_B < -20.5 - z$ or $M_V < -20$ zCOSMOS galaxies in $0.1 < z < 1$ is 0.53 or 0.46, respectively), the different redshift evolution of early-type galaxies in the clusters and groups indicates that in $0.4 < z < 1$, groups are the preferred environment for the morphological transformation of galaxies over clusters. Combining the nearby clusters from the Wide-Field Nearby Galaxy Cluster Survey with the $z = 0.5 - 1.2$ literature data, Poggianti et al. (2009) come to a similar conclusion: the morphological evolution since $z = 1$ is more pronounced in low-mass clusters than in massive clusters.

4.2. Evolution of the Morphological Fraction as a Function of the Properties of the Group

In the previous section we have seen the changes in the morphological mix of galaxies in groups over cosmic time. Comparison of the yellow and red points in the panels on the left sides of Figures 3 and 4 also suggests a dependence on the group properties, since the yellow points represent groups that extend to poorer levels than the red points, which represent galaxies in (rich) groups that have at least two members above $M_B < -20.5 - z$. Desai et al. (2007) have shown that morphological evolution of galaxies at $z < 1$ is stronger in lower mass clusters than in the most massive ones and there have been number of claims that the strongest evolution between $z \sim 1$ and $z \sim 0$ in the galaxy properties has been in the intermediate mass (e.g., Poggianti et al. 2006) or density (e.g., Smith et al. 2005) environments.

We can use the group corrected richness and measured velocity dispersion to study the morphological segregation as a function of a group property in our own sample. While the best way to isolate the effect of a group property would be to use galaxies in a narrow range of physical properties selected in a narrow bin of group properties, that type of analysis is not possible with the current 10k zCOSMOS sample due to the small number statistics. Therefore, we use instead the luminosity-complete samples of galaxies in groups of similar properties.

4.2.1. Group Richness

First, we look at the dependence of the morphological fraction of galaxies as a function of the corrected richness of the host group. We carry out this study for the four luminosity-complete samples defined above, using the group corrected richness defined in each of the luminosity-complete samples, i.e., the corrected number of members above the given galaxy luminosity limit. We split the group galaxies in bins using the corrected richness of a group (above the quoted luminosity limit) between 2 and 5, between 5 and 8 and larger than 8 for the groups in the luminosity-complete samples up to a luminosity of $M_B < -20 - z$. For the brightest sample $M_B < -20.5 - z$ we define bins of group corrected richness between 2 and 7 and larger than 7, considering only galaxies and groups in $0.4 < z < 1$ in order to keep the statistics meaningful. The results are shown in Figure 5. For lower luminosity galaxies, there is a clear trend for the richest groups to have a higher early-type fraction, especially as the redshift decreases.

4.2.2. Velocity Dispersion

This analysis can be repeated using the observed velocity dispersion for the groups. Due to the large uncertainties related to velocity dispersion measurements (see Knobel et al. 2009),

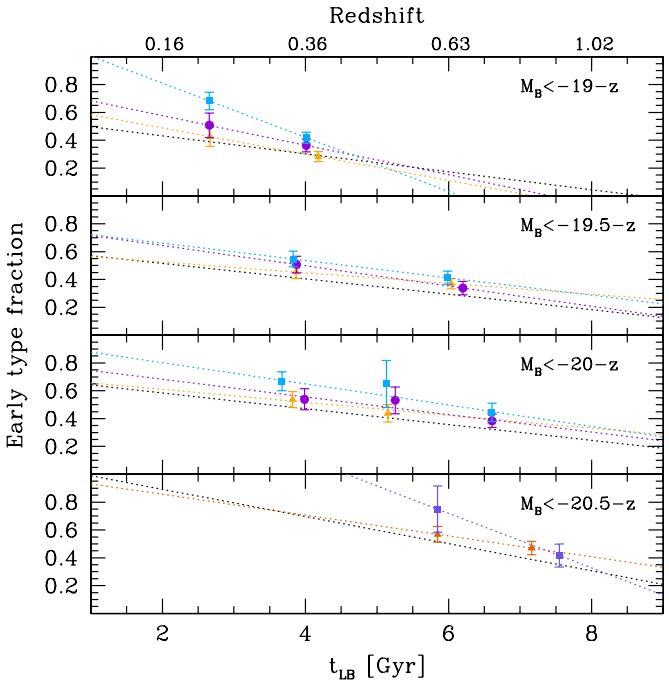

Figure 5. Time evolution of the fraction of early-type galaxies in groups of various richness. The solid symbols represent the group population in luminosity-complete samples as indicated in the individual panels, which are also used to define the corrected richness. The orange triangles, violet circles, and blue squares are for the galaxies residing in the groups with corrected richness between 2 and 5, between 5 and 8, and larger than 8, respectively, for the top three panels. In the bottom panel, the light red triangles and violet-blue squares are for the groups with corrected richness between 2 and 7, and larger than 7, respectively. The points are plotted at the median look-back time of galaxies in that bin. The dotted lines are the linear fits to the $f_{\rm early}$–t_{LB} relation for the various samples, marked in the same color as the corresponding early-type fractions. For a comparison, the dotted black line (without symbols) represents the linear fit to the $f_{\rm early}$–$t_{\rm LB}$ relation of the field galaxies in the corresponding luminosity-complete sample. At lower luminosities and/or lower redshifts there is a clear trend of higher early-type fraction in the richer groups.

(A color version of this figure is available in the online journal.)

only groups with at least five observed members (above the $I_{\rm AB} < 22.5$ cut) are used for this analysis. Using the four previously defined luminosity-complete samples of galaxies, we divide the groups into two sets according to their velocity dispersion: $250 < \sigma < 500$ km s^{-1} and $\sigma > 500$ km s^{-1}. The fraction of early-type galaxies in these two group bins is shown in Figure 6.

Even though this is of a lower significance, the same picture emerges as before. The fraction of early-type galaxies is larger in the groups with larger velocity dispersion for galaxies fainter than $M_B = -19.5 - z$. For brighter galaxies we do not detect any significant difference between fractions of early-type galaxies in groups of different velocity dispersion, possibly due to the limited number of galaxies.

4.3. Importance of the Stellar Mass Distributions (Stellar Mass Function in Groups and in Isolated Galaxies)

For comparison with the literature, the above discussion was based on the rest-frame B-band luminosity. As well as the obvious sensitivity of the B-band luminosity to the recent star formation history, there are many reasons to prefer stellar mass as a yardstick of galaxy properties. In particular, as mentioned in Section 1, the existence of a correlation between the stellar mass function of galaxies and their environment (Baldry et al. 2006;

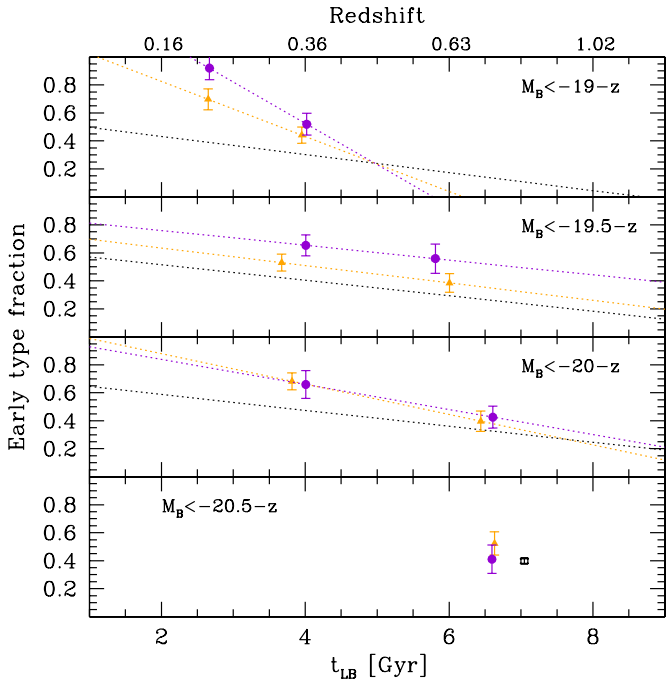

Figure 6. Fraction of early-type galaxies in different environments defined by the velocity dispersion of a group, as a function of redshift/time. The yellow triangles and violet circles are for the galaxies residing in groups with velocity dispersions between 250 and 500 km s^{-1}, and larger than 500 km s^{-1}, respectively. The additional requirement is that a group has at least five observed ($I_{AB} < 22.5$) members. In the given panels, all galaxies used for the analysis satisfy the indicated magnitude limit, and the redshift ranges in which these samples are complete. The points are plotted at the median look-back time of galaxies in that bin. The dotted lines are the linear fits to the f_{early}–t_{LB} relation for the various samples, marked in the same color as the corresponding early-type fractions. For a comparison, the dotted black line (without symbols) represents the linear fit to the f_{early}–t_{LB} relation of the field galaxies in the corresponding luminosity-complete sample. The bottom panel is an exception where we consider a sample of $M_B < -20.5-z$ galaxies only in $0.6 < z < 1$ in order to keep the number of galaxies statistically meaningful. For a comparison, we plot the fraction of early-type field galaxies measured in the same redshift range, marked with the black open square. The fraction of early-type galaxies is larger in the groups with larger velocity dispersion for galaxies fainter than $M_B = -19.5 - z$.

(A color version of this figure is available in the online journal.)

Bolzonella et al. 2009), plus the strong correlation between mass and galaxy properties, means that any sample that contains a significant range of masses may show a spurious environmental dependence simply because of the different distribution of masses in the different environments. This will be true not only for *B*-selected samples, but also *K*-selected samples, and even mass-limited samples (i.e., all galaxies with masses above some threshold). The spurious environmental effects produced by this difference in mass functions is shown by the clear flattening of the observed color–density and morphology–density relations (Cucciati et al. 2010; Tasca et al. 2009) when going from narrow M_B luminosity bins to narrow mass bins.

Using the overall zCOSMOS density field (Kovač et al. 2010), Bolzonella et al. (2009) have shown that the stellar mass functions of galaxies are different in different environments up to at least $z \sim 0.7$, and probably at higher redshifts. The galaxy stellar mass function in the densest regions, defined by the highest quartile in the distribution of galaxy environments at that redshift bin, is of bimodal shape at least up to $z \sim 0.5$, showing an upturn at low-mass end and with massive galaxies preferentially residing in these densest regions. Bolzonella et al. (2009) explain the environmental dependence of the shape of the stellar mass function by the different relative contributions of galaxies of different types in different environments. The individual stellar mass function for each of the different types is well represented by the Schechter function in all environments (see Figure 4 in Bolzonella et al. 2009). The higher contribution of the red/early objects in the densest environments produce a characteristic "bump" at high-mass end in the stellar mass function in the densest environment.

In this paper, we are investigating the morphological properties of galaxies in the group environment (Knobel et al. 2009), corresponding to virialized structures (i.e., single dark matter halos)—and can be confident from the comparison with the mocks that this is indeed to a large degree the case (Knobel et al. 2009). Not surprisingly, galaxies in the identified groups reside also in the denser environments (see Figure 22 in Kovač et al. 2010), and the groups are themselves good tracers of the dense peaks in the density field (see Figure 23 in Kovač et al. 2010). However, there is not a one-to-one correspondence between the group and the continuously defined environment.

We have therefore recalculated the stellar mass function for the samples of the group and isolated galaxies used in this paper, following exactly the same methodology as described in Bolzonella et al. (2009). The stellar mass functions are calculated using the $1/V_{max}$ method, by using the additional weights for each galaxy to correct for the average sampling and redshift success rate of the 10k HCC zCOSMOS sample to the full 40k sample (as the stellar mass function deals with the volume densities and not fractions of objects, similar to the weights used to define the group richness). The errors correspond to Poissonian errors obtained from the $1/V_{max}$ method. The V_{max} refer to the total zCOSMOS volume, and therefore the normalization of all stellar mass functions, except of the one of the total sample of galaxies, is arbitrary. As for the rest of the analysis in this paper, galaxies are selected to reside in the central zCOSMOS region, defined in Section 3.

The resulting stellar mass functions for the group and isolated sample of galaxies for four redshift bins are shown in the left and right panels in Figure 7, respectively (black symbols and curves). The mass functions are fitted with a double Schechter function (with a unique value of the exponential cut-off) in the two lower redshift bins and with a single Schechter function in the two higher redshift bins. To be able to compare similar group environments at different redshifts, we select only group galaxies residing in the groups with at least two corrected $M_B < -20.5 - z$ members. The shape of the stellar mass functions in the sample of group and isolated galaxies is reminiscent of the shape of the stellar mass functions in the sample of galaxies in the highest and lowest quartile of overdensities in Bolzonella et al. (2009). For the group galaxies, similar results are obtained when using all group members without restriction in the group richness—smoothing slightly the characteristic bimodal shape of the mass function in the dense region in the two lowest redshift bins, as expected when including in the galaxy sample also members of the smaller groups.

We also calculate stellar mass function per morphological type in different environments, using the morphological classification described in Section 2.5. As expected, the high mass end of the stellar mass function in both environments is dominated by early-type galaxies, peaking at roughly $10^{11}\ M_{\odot}$. Toward lower masses, the number of early-type galaxies decreases and the number of late-type galaxies increases. Late-type galaxies

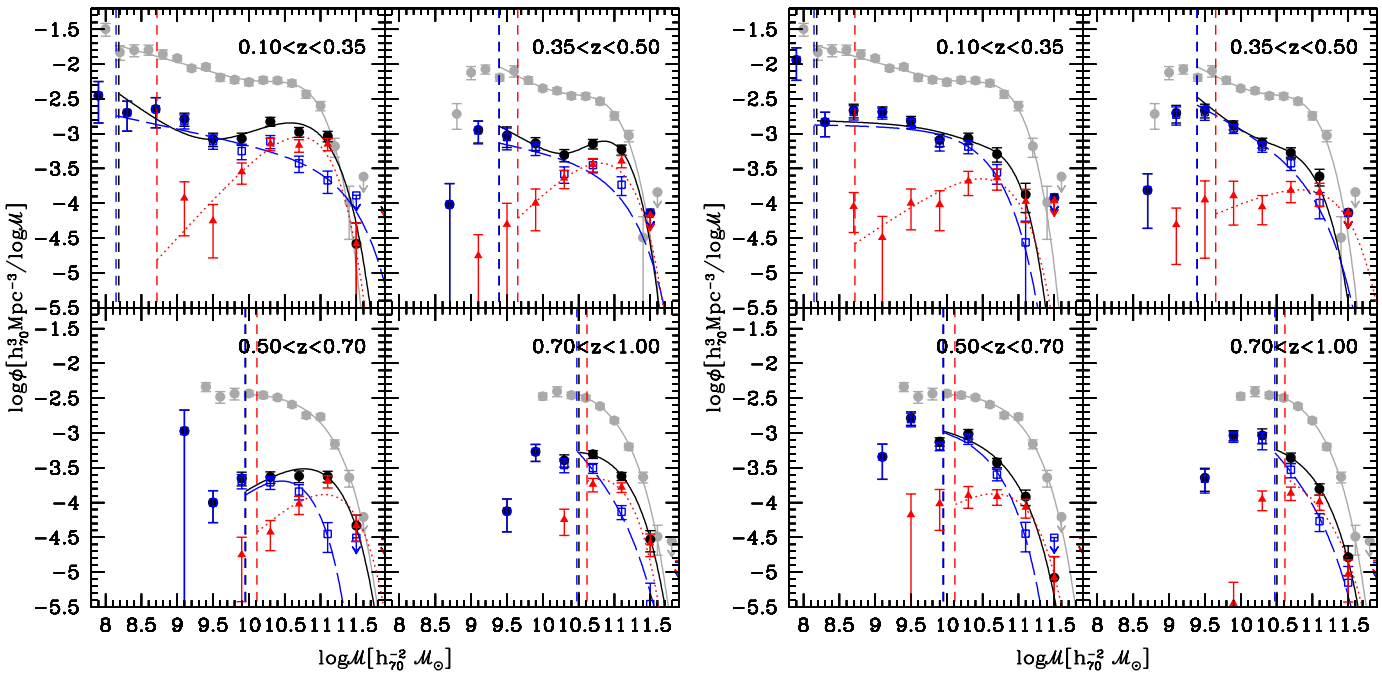

Figure 7. Stellar mass function in different environments. The left-hand panels are obtained for the group galaxies residing in the groups with at least two corrected $M_B < -20.5 - z$ members. The right-hand panels are for the isolated galaxies. The symbols correspond to the $1/V_{\rm max}$ measurements and the continuous lines correspond to the Schechter fits (see text for more details). Each four-panel figure covers $0.1 < z < 1$, split in four redshift bins indicated on the top. The black, red, and blue symbols/curves are results for the populations of all, early-type, and late-type galaxies, respectively. For a comparison, the stellar mass function of the field galaxies is presented with gray symbols/curve. The environmental dependence of the shape of the stellar mass function is explained by the different relative contributions of galaxies of different types in different environments. See Bolzonella et al. (2009) for the detailed discussion of the role of environment on the stellar mass function.

Table 2
Number of (Non-weighted) Galaxies in the Mass-complete Samples

$M_{*,\rm compl}$ Limit z Range	$\log(M_*/M_\odot) > 9.88$ $0.1 < z < 0.45$	$\log(M_*/M_\odot) > 10.21$ $0.1 < z < 0.6$	$\log(M_*/M_\odot) > 10.68$ $0.1 < z < 0.8$	$\log(M_*/M_\odot) > 10.96$ $0.2 < z < 0.95$
Group($M_B < M_{B,\rm compl}$)	422	390	294	132
Group($M_B < 20.5 - z$)	241	235	218	132
Field	987	1045	858	428
Isolated	141	180	109	40

dominate below the crossing mass (the mass at which the two mass functions cross) and this crossing mass shifts toward lower values at later cosmic epochs. Since $z \sim 0.7$, the crossing mass is clearly lower for the group than the isolated sample of galaxies. We will discuss the crossing mass in more detail in the following sections.

We therefore find that the stellar mass function exhibits a similar shape dependency on environment, whether environment is defined as a continuous field (density of objects) or a discrete (groups/isolated sample) quantity. Moreover, the reason is the same: the different relative contributions of galaxies of different types across a range of masses (see Bolzonella et al. 2009 for more discussion).

We stress that one consequence of this for any analysis related to the environment, is that whenever there is a sample of galaxies that contains a range of stellar masses, then the relationships between a given galaxy property and environment will be modulated by the relationship between that property and stellar mass through the differing mass distributions of galaxies with environment. To isolate the true environmental effect, we must consider galaxies in narrow stellar mass bins.

4.4. Morphological Mix in Different Environments from the Mass-selected Samples

We therefore select four stellar mass-complete samples of galaxies to investigate the morphological mix inside and outside groups in zCOSMOS. The selection of the complete stellar mass samples has been described in Pozzetti et al. (2009), and is optimized to be complete for both early- and late-type galaxies following our definition of morphological types. We use the samples that are 85% complete for the early-type (1+2.0) galaxies. The samples are defined as follows: $\log(M_*/M_\odot) > 9.88$ in $0.1 < z < 0.45$, $\log(M_*/M_\odot) > 10.21$ in $0.1 < z < 0.6$, $\log(M_*/M_\odot) > 10.68$ in $0.1 < z < 0.8$, and $\log(M_*/M_\odot) > 10.96$ in $0.2 < z < 0.95$. The numbers of galaxies in the different environments within these mass-complete samples are given in Table 2.

The morphological mix of galaxies within these mass-selected samples in different environments is shown in Figure 8. The stellar mass bins have a width of $\Delta \log(M_*/M_\odot) = 0.7$ (dictated by the number statistics), starting from the lowest stellar mass for which the samples will be complete. This means our

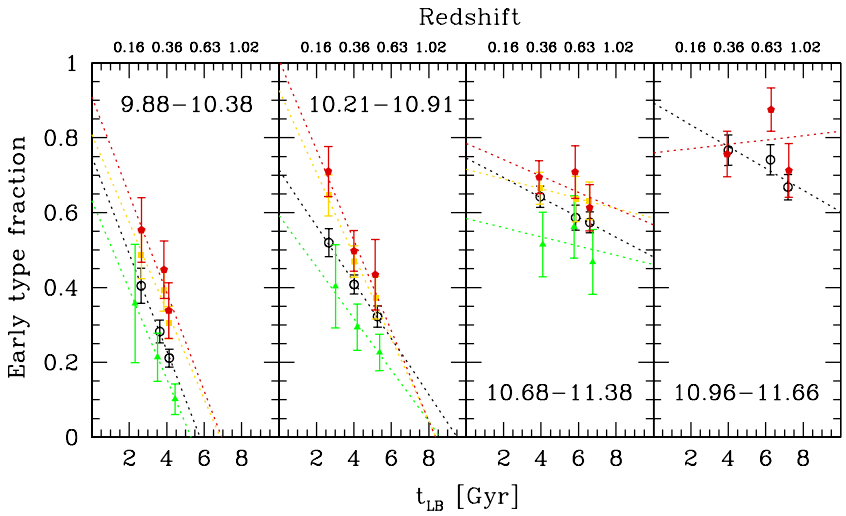

Figure 8. Redshift evolution of the fraction of early-type galaxies of a given stellar mass in different environments. The stellar masses are from intervals of $\log(M_*/M_\odot) = 0.7$ width, where the interval limits in $\log(M_*/M_\odot)$ units are given in the individual panels. The lower stellar mass value represents the 85% completeness limit for the early (1 + 2.0) type galaxies in the redshift interval of consideration: $0.1 < z < 0.45$, $0.1 < z < 0.6$, $0.1 < z < 0.8$, and $0.2 < z < 0.95$ going from the left to the right, respectively. The solid yellow squares and solid red pentagons represent group galaxies with the corrected richness of at least two in the corresponding luminosity complete sample and in the $M_B < -20.5 - z$ sample of galaxies, respectively. The empty black circles represent the field galaxies and the green solid triangles represent the isolated galaxies. The symbols are plotted along the horizontal axis at the median look-back time/redshift of galaxies in the considered bin. The dotted lines are the linear fits to the $f_{\rm early}$–$t_{\rm LB}$ relation for the various samples, marked in the same color as the corresponding early-type fractions. For galaxies with $\log(M_*/M_\odot) \lesssim 11$, there is a steady increase with cosmic time in the fraction of early-type galaxies in all environments. Moreover, the fraction of early-type galaxies is highest in the group environment, and lowest for the isolated galaxies at every redshift probed by that particular $\log(M_*/M_\odot) \lesssim 11$ stellar mass.

(A color version of this figure is available in the online journal.)

mass bins are partially overlapping, and consequently, not independent of each other.

For the stellar masses below $\sim \log(M_*/M_\odot) = 11$ we observe a steady increase with cosmic time in the fraction of early-type galaxies in all environments. For the highest mass bin, $10.96 < \log(M_*/M_\odot) < 11.66$, the number of galaxies is small, and little can be conclusively said regarding the groups and for the field. However, it seems clear that high fractions ∼70%–80% of early-type $\sim \log(M_*/M_\odot) > 11$ galaxies in both the group and field are present before $z = 1$ and that the morphological mix stays more or less constant since then.

Progressing to lower masses, we find that, at a given stellar mass, the fraction of early-type galaxies is consistently highest in the group environment, and lowest for the isolated galaxies, at every redshift that we can examine for that particular stellar mass. Fitting a linear relation between the early-type fraction and look-back time, the linear fits for galaxies with $\log(M_*/M_\odot) \lesssim 11$ suggest that the fractions of early-type galaxies were more or less the same in all types of environment at higher redshifts and then, with cosmic time, diverged with progressive morphological transformation from late- to early-type galaxies happening at different rates in different environments at a given mass. As noted above, there is an indication that the increase in the early-type fraction over cosmic time is more rapid in the groups with higher richness than in the poorer groups (e.g., difference between red pentagons and yellow squares and the corresponding linear fits in Figure 8).

Looking at the same data from another perspective, we can calculate the fractions of early-type galaxies as a function of stellar mass in the narrow redshift bins: $0.2 < z < 0.4$, $0.4 < z < 0.6$ and $0.6 < z < 0.8$. These are shown in Figure 9, using only groups with a corrected richness of at least two in the $M_B < -20 - z$ sample, as we extend this analysis only to $z = 0.8$. At every redshift, the fraction of early-type galaxies increases strongly with the stellar mass for galaxies residing in both the groups and in the field. The isolated galaxies follow

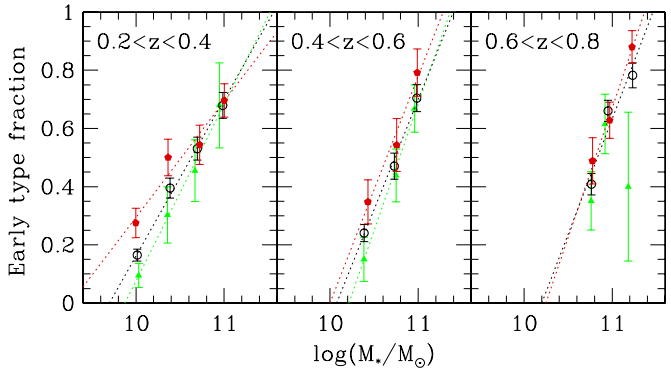

Figure 9. Environmental dependence of the fraction of early-type galaxies on stellar mass. The red solid pentagons represent the group galaxies with the corrected richness of at least two in $M_B < -20 - z$ sample of galaxies, the empty black circles represent the field galaxies, and the green solid triangles represent the isolated galaxies. In the selected redshift intervals, galaxies are extracted from the stellar mass-complete samples (85% completeness limit for the early 1+2.0 type galaxies). The symbols are plotted along the horizontal axis at the median mass of galaxies in the considered bin. The dotted lines are the linear fits to the $f_{\rm early} - \log(M_*/M_\odot)$ relations, marked in the same color as the symbols in the corresponding environments. At every redshift, the fraction of early-type galaxies increases strongly with the stellar mass for galaxies residing in both the groups and in the field. The morphological mix that is achieved in the groups at some redshift and at some mass, is achieved at only slightly later times (or equivalently for slightly higher masses) in the field and for the isolated galaxies.

(A color version of this figure is available in the online journal.)

the same trend in the lowest redshift bins up to $z = 0.6$, while in the highest redshift bin they become very rare objects and the obtained statistics is much less reliable. This figure also illustrates the convergence of the morphological mix at a given (relatively high) mass at redshifts approaching $z \sim 1$.

These results are in good agreement with Tasca et al. (2009), who showed the weakening of the overall morphology–density relation at high stellar mass and/or high redshifts in similar

mass-complete samples in the zCOSMOS. However, the increase of the early-type fraction with stellar mass in $0.2 < z < 0.8$ (Figure 9) contrasts with results obtained by Holden et al. (2007), who do not detect any clear trend in the early-type fraction with stellar mass for the cluster galaxies more massive than $\log(M_*/M_\odot) = 10.52$. We have taken into account the difference in the initial mass function (IMF) used by Holden et al. (2007) and here, assuming that the stellar masses calculated with the Chabrier IMF are larger by 0.08 than the "diet Salpeter" IMF used by Holden et al. (2007; see, e.g., Bolzonella et al. 2009 on the differences between the stellar masses with different IMFs). Holden et al. (2007) results are obtained for five massive X-ray clusters in $0.023 < z < 0.83$ spanning a range in velocity dispersion 865 km s^{-1} $< \sigma <$ 1156 km s^{-1}, or with 56 to 109 members above the quoted mass limit. The measured fractions of early-type galaxies are between 71% and 100%, comparable to the fractions we measure only for the most massive $> \log(M_*/M_\odot) \sim 11$ galaxies. This indicates that clusters are either more efficient in transforming late-types to early-types or that the bulk of morphological transformation of galaxies more massive than $\log(M_*/M_\odot) = 10.52$ has happened earlier in the clusters than in any other environment, and specifically the poorer group environments examined here.

Figures 8 and 9 also show one way of looking at the relative importance of mass and environment in driving morphological transformation. It can be seen that the morphological mix that is achieved in the groups at some redshift and at some mass, is achieved at only slightly later times (or equivalently for slightly higher masses) in the field (all galaxies) and in the isolated galaxies. At $z \sim 0.5$ and $\log(M_*/M_\odot) \sim 10.2$, the "effect" of group environment is equivalent to only about 0.2 dex in stellar mass or to about 2 Gyr in time.

Fitting the linear relation to the observed $f_{\rm early} - \log(M_*/M_\odot)$ trends at a given redshift bin, we can calculate the stellar mass at which 50% of galaxies in a given sample is of early-type at that redshift. We call this quantity the morphological crossing mass since it is also obviously the mass at which the individual mass functions of the two populations cross. The change with redshift of the morphological crossing mass in the group and other environments is shown in Figure 10. The morphological crossing mass decreases with decreasing redshift, indicating that the morphological transformation from late to early-types starts in galaxies with higher stellar masses and shifts to galaxies with lower stellar masses over cosmic time. This is another manifestation of the so-called downsizing scenario in the evolution of galaxies (e.g., Cowie et al. 1996). At $z \sim 0.7$ or a little above, 50% of galaxies with masses of $\log(M_*/M_\odot) \approx 10.85$ are already of early-type, independent of their environment. Moving toward lower redshifts, the morphological crossing mass decreases more rapidly for galaxies residing in groups than for the field and isolated galaxies reflecting the emergence of morphological segregation.

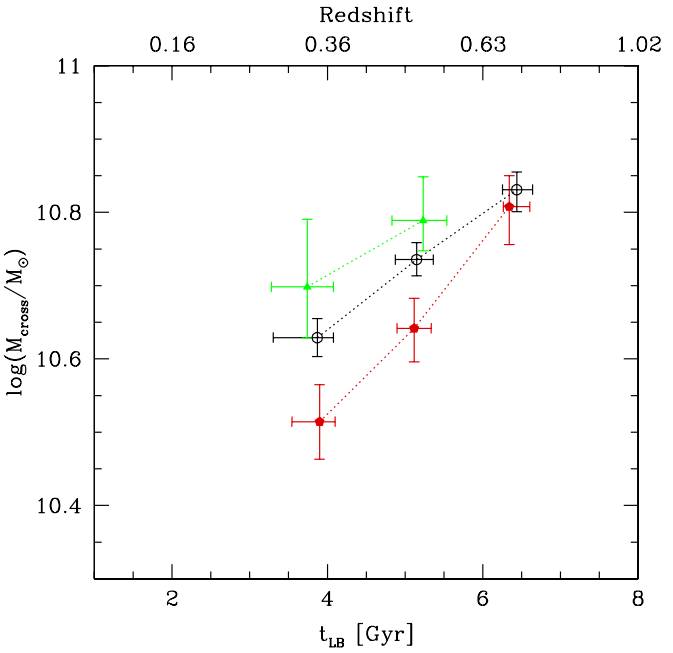

Figure 10. Morphological crossing mass of galaxies in different environments. The red solid pentagons represent the group galaxies, the empty circles represent the field galaxies, and the green solid triangles represent the isolated galaxies. The crossing mass is the mass at which 50% of the selected galaxy population is of early (or equivalently of late) type. The values of the crossing masses are estimated from the linear fits to the measured points in Figure 9 in the individual redshift intervals. The vertical error bars correspond to the rms values in the crossing mass obtained by bootstrapping of the galaxy samples and repeating the fitting, using the previously estimated errors on the real fractions. The horizontal error bars correspond to the upper and lower quartiles in the look-back time distribution of galaxies in the considered redshift bins, plotted at the median look-back time/redshift in that bin. The morphological crossing mass decreases with decreasing redshift, indicating that the morphological transformation from late- to early-types starts in galaxies with higher stellar masses and shifts to galaxies with lower stellar masses over cosmic time. Moving toward the lower redshifts, the morphological crossing mass decreases more rapidly for galaxies residing in groups than for the field and isolated galaxies.

(A color version of this figure is available in the online journal.)

5. DISCUSSION

5.1. The Relative Role of Stellar Mass and Environment in Determining Galaxy Properties

The above results have painted a consistent picture of a morphological segregation emerging between the typical group and field environments (i.e., all galaxies) emerging over the last several billion years, since $z \sim 1$, and of being more prominent in galaxies of lower luminosity and/or stellar mass. Corresponding trends in the zCOSMOS 10k sample relative to the larger scale density field were shown in Tasca et al. (2009).

On the one hand, it is clear that this emerging environmental dependence is superposed on top of a global and strong mass-driven evolution that is seen in the whole population. There is no doubt that the stellar, or possibly total baryonic, mass ("nature") is directly related to the processes responsible for this morphological transformation. The offset between the observed fractions of different morphological types of galaxies in different environments since $z \sim 1$, i.e., higher fractions of early-type galaxies for the group than the typical field population, which are again higher than the fractions for the isolated galaxies (Figure 8), is, however, tuned by the environment. As noted above, at a given mass, this environmental tuning corresponds to about 2 Gyr in time: a certain morphological mix, a product of the efficient morphological transformation, will be achieved first in the group, then in the field and at the end in the isolated environments for galaxies of a given mass.

However, it is not immediately clear if this is because of an offset in "starting time," as the more massive galaxies are expected to be formed first in the more massive structures (again "nature," e.g., Kauffmann 1995; Benson et al. 2001; Heavens et al. 2004), or because of a difference in the rate of evolution in different environments ("nurture"), caused by some

of the dense environment related processes (e.g., ram pressure stripping, harassment, etc., see Section 1).

Moreover, we do clearly detect an apparent increase in the environmental differences, at least for lower mass galaxies which are transforming at lower redshifts. This produces the clear divergence of the morphological crossing masses from $z \sim 0.7$ to $z \sim 0.3$ in different environments, suggesting that the morphological transformation rate is rather faster in the groups than outside of them. However, an interpretation of Figure 10 in terms of the physically relevant processes is not trivial, since it also reflects both the shape of the mass functions and their relative amplitudes in different environments.

We therefore investigate the rates of the morphological transformation more directly. It is also of interest to compare the transformation rates for other relevant transformations, and specifically those related to the star formation history, i.e., the "quenching" transformation from blue to red, or from active star formation to passive evolution. Of course, all of these processes may be reversible, and so we are really looking at the "net" transformation rate. Comparison of these transformation rates may provide clues as to the physical linkage between morphological transformation and star formation quenching.

5.2. Timescales for Type Transformations of Galaxies

One interesting question regarding morphological transformation and star formation quenching is whether one preceded the other. Based on the field stellar mass functions of the zCOSMOS galaxies of different types, Pozzetti et al. (2009) find that the morphological crossing mass has higher values than the equivalently defined crossing mass for the populations of photometrically red and blue, and also active and passive galaxies. From the differences in the number density of photometrically and morphologically early-type galaxies, the inferred delay time between the color and morphological transformation is about 1–2 Gyr. A similar timescale is derived for the transformation to red colors after a switch in the star formation. Bundy et al. (2006) qualitatively find the same behavior for the crossing mass of the DEEP2 field galaxies when the population of galaxies is split according to the morphology and color, extending the color/morphology dichotomy of crossing mass to redshift 1.4.

Similar results have been obtained for the population of cluster galaxies. Wolf et al. (2009) study the population of galaxies in the A901/2 cluster complex at $z \sim 0.17$, finding the majority of high mass galaxies (above $10^{11}\,M_{\odot}$) to be red and spheroidal in all environments (outskirt, center, and outside of cluster). Based on the large number of cluster spirals in the mass range of 10^{10}–$10^{11}\,M_{\odot}$, Wolf et al. (2009) conclude that quenching of star formation in these galaxies is a slow process, where the timescale of morphological evolution must be longer than that of the spectral evolution. However, at even lower masses, not accessible by our study, decline in star formation rate and morphological changes appear to be more synchronized in A901/2. Using the sample of 24 clusters from the EDisCS (White et al. 2005), Sánchez-Blázquez et al. (2009) find that the fraction of early-type red sequence galaxies decreases by ∼20% from $z = 0.75$ to $z = 0.45$, which can be expected if the cluster spiral galaxies first get redder, stopping their star formation, before they become early-type (note that Sánchez-Blázquez et al. 2009 have done the analysis using the luminosity-complete samples).

Using the marked correlation statistics on the Sloan Digital Sky Survey (SDSS) data, Skibba et al. (2009) conclude that $z \sim 0$ red spirals are often satellites in the outskirts of groups and clusters, while red early-type galaxies are preferentially located in the centers of these structures. Skibba et al. (2009) suggest that the timescale of the morphological transformation of these red spirals is longer than that of the quenching of their star formation. The zCOSMOS extends a high-redshift (up to $z \sim 1$) comparison between the color and morphological properties of galaxies to the group environment.

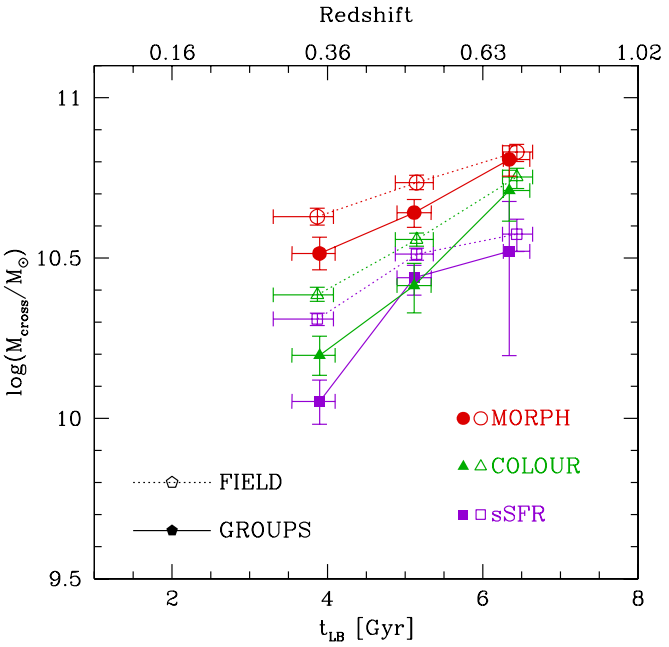

Figure 11. Evolution of the class-dependent crossing mass in the group and field environments. The filled symbols are for the group and the empty symbols are for the field samples. The red circles, green triangles, and violet squares correspond to the morphological, color and star-formation activity crossing mass, respectively. Error bars for each value have been estimated following the same procedure described in the caption of Figure 10. The effective transformation of galaxies from active to passive, from blue to red, and from late to early moves progressively toward lower mass galaxies as cosmic time passes or as the environment is denser. The crossing masses for morphology are higher, and change less rapidly, than those for color and/or star formation activity.

(A color version of this figure is available in the online journal.)

To enable a closer comparison between the color and morphological properties of galaxies in the group environment, we calculate the color crossing mass using the same procedure and the same galaxy samples that were used to calculate the morphological crossing mass, described in Section 4.4 (see also Iovino et al. 2010 who calculate a similar quantity, t_{50-50}, the cosmic time at which the fraction of red/blue galaxies is 50%). In addition, we also calculate the crossing mass for star formation activity by partitioning galaxies into active and passive classes using the specific star formation rate (sSFR) from the SED fitting (see discussion in Pozzetti et al. 2009 on the agreement between the star formation rates derived from these SEDs and those from measurement of emission lines). In this work, we consider galaxies with $U - B > 1.1$ to be red, and galaxies with $\log(\mathrm{sSFR/yr}) < -10.5$ to be passive. These crossing masses for the group and field samples are shown in Figure 11.

The crossing mass for each of the samples shows behavior similar to what we have already shown for the morphological crossing mass. It shifts to lower masses with cosmic time in both the field and group environment, and since $z \sim 0.6$, this evolution is clearly environment dependent. The activity crossing mass is systematically lower than the color crossing

mass, which is systematically lower than the morphological crossing mass. This is observed both in the field (in agreement with Pozzetti et al. 2009) and in the group environment. Extrapolating the plot, at a given mass 50% of the population will turn passive at an earlier cosmic time than the time at which 50% of the population will become red. Fifty percent of the population will become early morphological type even later. Moreover, this will generally happen earlier for a group galaxy than for a field galaxy. A similar sequence of the color and morphological crossing mass in the zCOSMOS has been presented in Bolzonella et al. (2009) for the environments of extreme densities, when quantifying environment using the local overdensity of neighboring galaxies (Kovač et al. 2010). Bundy et al. (2006) find tentative evidence for the rise of the quiescent population in dense, continuously defined environments.

While the exact values of the crossing mass are strongly dependent on how galaxies were divided into types, there is a clear and progressive (with epoch) environmental dependence in these values. The effective transformation of galaxies from active to passive, from blue to red, and from late to early moves progressively toward lower mass galaxies as cosmic time passes or as the environment is denser. Derived values of the various crossing masses are consistent with a scenario in which, for the majority of galaxies, the timescale for the morphological transformation is longer than the timescale for the color transformation, both in the field and group environment, assuming that all these processes started to act approximately at the same time in a given environment.

Unfortunately, it is hard to use arguments such as the location and rate of change of the above-defined crossing mass to infer quantitative information on the transformation rates, since these may be sensitive to the choice of the location of the dividing line between the two properties and also on the shape and relative normalization of the mass functions of different components of the population. The dividing line may be clear for color (e.g., the so-called "green valley") but more arbitrary in the case of morphological classification. The relative amplitude of the mass functions of early- or late-type galaxies, and of blue or red galaxies, or of active or passive galaxies, will also change the location and movement of $M_{\rm cross}$. Use of the redshift/epoch axis to determine transformation rates, i.e., of the flux of galaxies crossing through a chosen dividing line, is likely to be less sensitive to the precise location of that divide and to allow a more direct study of these questions.

5.3. Role of Group Environment in the General Galaxy Type-Transformation Rate

In the following, we explore more directly the "transformation rate" of late-type galaxies into early-type galaxies for different masses and different environments in order to try to better understand the physical causes. It should be noted in the following discussion that this is really a "net" transformation rate from late to early, since it is in principle possible for early-type galaxies to reacquire a gaseous disk and become of later morphological type, although whether this would be sufficient to cross our defined morphological divide between ZEST classes 2.0 and 2.1 is unclear.

Assuming from now on that galaxy transformations are dominated by one-way transformation from late to early (and blue/active to red/passive), we proceed to define a normalized transformation rate η in which the rate of change in the number of "progenitor" galaxies (either late-type, blue, or active) is normalized by the number of these progenitors:

$$\eta = -\frac{1}{N_C}\frac{dN_C}{dt} = -\frac{d\ln N_C}{dt}, \quad (5)$$

where N_C is a measure of the number of progenitors of a given class C, i.e., the mean comoving density averaged over suitably large volumes of the universe.

The inverse of η gives the transformation timescale t_η for a typical "progenitor galaxy" to be transformed. The transformation rate η might be expected to be a function of mass, environment, and probably epoch.

Unfortunately, an accurate determination of $N_C(z)$ and dN_C/dt for a particular class C of galaxies is observationally challenging. It requires an accurate measurement of galaxy properties, e.g., the stellar mass, over a range of redshifts, careful treatment of large-scale density variations within surveys due to large-scale structure, and, ideally, knowledge of the changes in the number of galaxies in a particular class due to, for instance, mass growth through star formation and/or merging. In the case of galaxies defined by environment, i.e., those in groups, there will also be a change in the population due to the hierarchical growth of the groups through the accretion of galaxies onto the virialized structures.

In cases where it can be assumed that the total number of galaxies in a given bin (defined by mass and environment) is more or less constant, then some of these difficulties can be alleviated by considering the fraction of galaxies, rather than their absolute number, i.e., by dividing by a fixed total number of galaxies N. In this case,

$$\eta = -\frac{1}{f_C}\frac{df_C}{dt} = -\frac{d\ln f_C}{dt}. \quad (6)$$

If the evolution of $\ln f_C$ is linear with cosmic time, we simply obtain η as the slope to this relation for any sample defined by mass and environment. With the limited baseline in redshift and limited number statistics, we will henceforth consider the rate η as single time-averaged rate over the accessible range of epochs, from a linear fit to $\ln f_C$–t.

For group galaxies, we know that the total number of galaxies is certainly not conserved, because galaxies will be accreting onto the group from the surrounding regions. It is clear that this migration into the groups is likely to further amplify any environmental difference in transformation rates, because the new arrivals will have to "catch up" with the existing group members which already have a more evolved state.

In the following, we derive a simple first-order correction accounting for the galaxies infalling to the groups by assuming (1) that the total number of galaxies in the sample (at a given mass) is conserved, i.e., we do not consider galaxy mergers and neglect the effects of star formation, and (2) that the infalling galaxies can be considered to be a representative subset of the non-group population. This latter condition may not be true, and this infall correction is therefore likely to represent an upper bound to the actual transformation rate.

In some small increment of time dt, the number of class transformations dN in groups will be given by

$$dN = -N_G df_{CG} - (f_{CG} - f_{CN})dN_G \quad (7)$$

where N_G is a number of the group galaxies, f_{CG} and f_{CN} are fractions of the C-class galaxies in the groups and non-groups, respectively, and where the class C is a "progenitor" type of

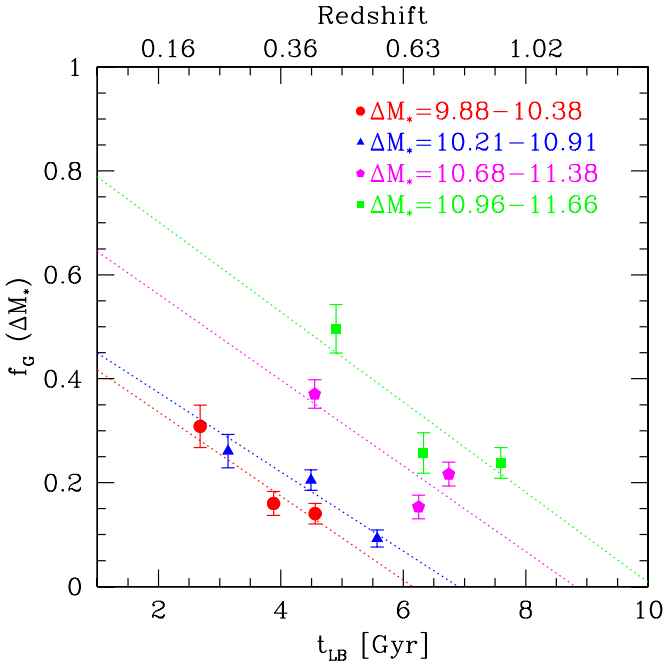

Figure 12. Evolution of the fraction of galaxies in our group sample (corrected richness of at least two in $M_B < -20 - z$ sample of galaxies). Different symbols correspond to the different $\Delta\log(M_*/M_\odot)$ mass bins, indicated in the right corner of the plot (omitting "log" and units in the indication of mass bins for clarity). The dotted lines are the linear fits to the time evolution of the fractions of group galaxies, extrapolated to all epochs. At a given stellar mass, the fraction of galaxies residing in the group environment increases with cosmic time, as individual groups grow through infall.

(A color version of this figure is available in the online journal.)

galaxy (i.e., assumed to be late morphological type or active/blue type). The equation above can be further written as

$$dN = -d(N_G f_{CG}) + f_{CN} dN_G. \quad (8)$$

By normalizing the number of transformations with $N_G f_{CG}$, which is the "pool" of potential objects in the group to be transformed, the rate $\eta_{\rm IN,CORR}$ including the effects of infall can be written as

$$\eta_{\rm IN,CORR} = -\frac{1}{f_{CG}}\frac{df_{CG}}{dt} + \left(\frac{f_{CN}}{f_{CG}} - 1\right)\frac{1}{f_G}\frac{df_G}{dt}. \quad (9)$$

In the case of no infall, where f_G is constant over time, or in the case where the group and non-group populations have the same properties at a given epoch, it can be seen that the rate η will be given just with the first term on the left-hand side, which is the same as Equation (6) above.

What about progenitor bias? By considering two simple complementary categories, group and non-group, and the change in the fraction of galaxies associated with each, we automatically deal with both additional membership of pre-existing groups and the emergence of new groups where none previously existed (above the fixed threshold in richness). We should, however, recognize that the rates so derived will be averages across the entire, evolving, group population and not, necessarily, representative of what is happening within a single group. Because of the attraction of using two complementary populations, group and non-group, we no longer consider either the isolated galaxies nor the field (all galaxies) populations in this analysis.

It is important to note that, based on extensive comparisons with the mock catalogs, neither the completeness nor purity of the group catalog are believed to depend significantly on redshift (Knobel et al. 2009, see Figure 9). The same is also true of the individual group members. This allows us to use the observed fraction of galaxies in a volume-limited sample of groups as a good estimate of the infall rate from the non-group into the group population, and the observed morphological mix of galaxies in and outside of those groups as representative of both populations. The redshift evolution of the fraction of galaxies residing in the groups with at least two corrected members above $M_B < -20.5 - z$ is shown in Figure 12. At a given stellar mass, the fraction of galaxies residing in the group environment increases markedly with cosmic time, building up these structures. At a given time, a larger fraction of the more massive galaxies are already present in the groups reflecting the different mass functions shown above (see Section 4.3 and Figure 7).

The derived rates of the morphological transformation $\eta_{L->E}$ in the group environment are shown in the left-hand panel in Figure 13. We obtain the infall corrected rates taking for the term $\frac{f_{CN}}{f_{CG}}$ the average of the measured fractions at different times at a given mass, discussed in Section 4.4 (see Figure 8). The errors are obtained by the error propagation of Equations (6) and (9), using the individual bootstrap errors on the fractions. The red filled circles represent the rates corrected for infall using Equation (9), while the red open circles represent those computed directly from Equation (6), which are lower, as expected. The equivalently derived rates for the non-group galaxies, which are galaxies not residing in groups with the corrected richness of at least two $M_B < -20.5 - z$ members, are shown in the right-hand panel in Figure 13 (red filled circles). We use the simple Equation (6) above, since the infall is a one-way depletion of the non-group population, again assuming that the infalling migrants are representative of the population as a whole.

In a similar manner, we derive the rates of the color transformation from blue to red galaxies $\eta_{B->R}$ and from active to passive galaxies $\eta_{A->P}$ using the same group and non-group samples of galaxies as for measurements of $\eta_{L->E}$. Galaxies are divided in different classes as in the previous subsection. The corresponding rates are overplotted in Figure 13 (using the green triangles for $\eta_{B->R}$ and violet squares for $\eta_{A->P}$). Generally speaking, the rates obtained for the color and activity class transformation also show similar dependence on the mass and environment as the rates of the morphological transformation.

Comparison of the two panels of Figure 13 shows three interesting facts. (1) The rate of the class transformation is consistently higher in the group environment than outside of it. (2) The rate of transformation is consistently higher for the transformations involving star formation than for those involving morphological transformation. (3) The rate is higher for lower mass galaxies than for higher mass ones. Indeed the rates, and the differences between the rates inside and outside of groups, and between morphology and star formation, are all small and consistent with zero for the most massive galaxies above $\log(M_*/M_\odot) \sim 11.2$. It should be noted that these rates must fall at still lower masses, beyond the range explored by zCOSMOS.

For typical galaxies with $\log(M_*/M_\odot) \sim 10.5$, we conclude that the transformation rates are three to four times higher in the groups than outside, and are typically 50% higher for color transformations than for morphological ones. The implied transformation timescales η^{-1}, are of order 1.8 Gyr (color transformation) or 2.5 Gyr (morphology transformation) in the

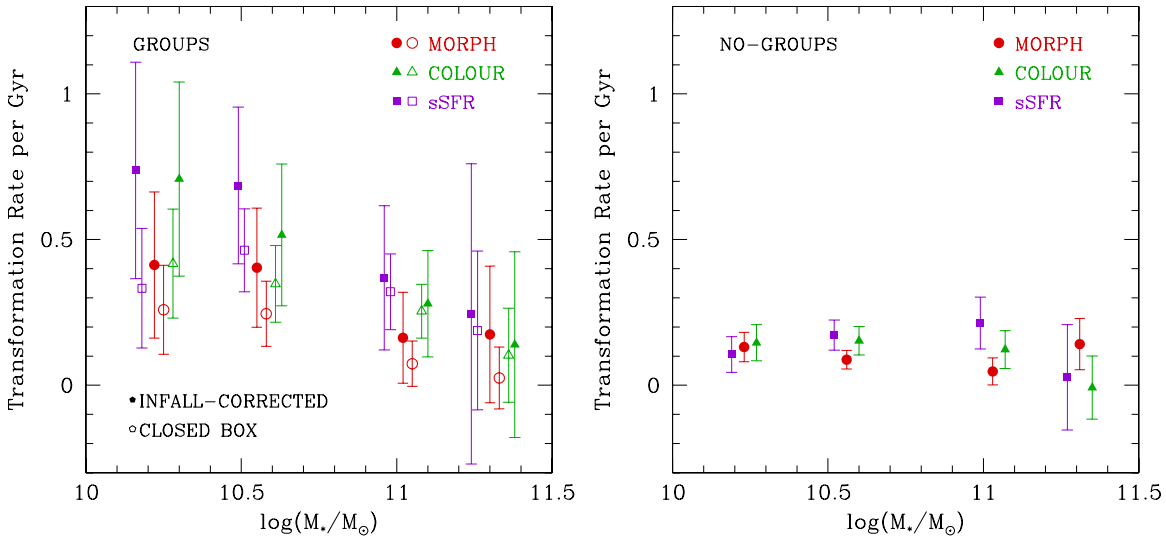

Figure 13. Derived transformation rates for morphology, color, and star formation activity in the group environment (left) and in the non-group environment (right). The solid symbols correspond to the final rates, which are corrected in the case of the group galaxies, for the infall of new members onto existing groups and the appearance of new groups above the selection threshold (see Equation (9)). It should be noted that this is "worst-case" correction which assumes that the new group members are representative of the previous non-group population. Using this same assumption, the rates in the non-group population need not be corrected for the loss of these galaxies (see Equation (6)). The open symbols in the left-hand plot correspond to the rates in the groups with no infall correction applied (Equation (6)). The morphological, color, and star formation activity rates are shown with the red circles, green triangles, and violet squares, respectively. The transformation rates are consistently higher in the group environment than outside of it. The rate of transformation is also consistently higher for the transformations involving star formation than those involving morphological transformation. Finally the rate is higher for galaxies around $10^{10.5}$ $M_{\odot}$ than for higher mass ones. The rates must also fall again at lower masses, which cannot yet be studied.

(A color version of this figure is available in the online journal.)

groups, and about 6 Gyr and 10 Gyr, respectively, outside of groups.

Needless to say, the exact values of the derived rates and corresponding timescales should be taken as indicative only. The quoted errors include only the purely statistical uncertainty. There are various other issues which one needs to be aware of. Although we have tried to deal with variations in $N(z)$ due to the large-scale structure by considering fractions, the temporal gradients may be affected by the choice of redshift bins, since this will be affected by large-scale structure. At low z, the volume used for the analysis is the smallest, and the estimated fractions could be less representative of the universal values than the fractions estimated at higher redshifts, modifying the true slopes in the overall fractional evolution. Moreover, we have assumed constant rates (i.e., a linear evolution in the logarithmic fraction), and have furthermore estimated these at different epochs for the different mass ranges. We believe that the relative values should be more robust than the absolute ones.

It is fairly clear, e.g., comparing Figures 7 and 8, that the difference in the transformation rates computed here stem as much from the different fractions in the different environments (in the denominator) as from differences in the rate of change of the fractions (in the numerator), which are often rather similar. It is also clear that this difference in the fractions between the different environments amplifies the difference in implied transformational rates in the groups through infall correction, increasing the difference by about ∼50%. However, it is clear that this is not the sole origin of the rate difference between the different environments.

It should be noted that there are at least two effects that would act to reduce the observed rates, and therefore lead us to underestimate the effect of the group. First, as noted earlier in the paper, the non-group galaxies as we define them here, will be somewhat "polluted" by galaxies in small groups that are not yet detectable in the relatively sparse sampled zCOSMOS 10k sample. This will tend to wash out the environmental differences. This contamination will arise from the non-perfect isolation of the group sample in terms of the imperfect purity and completeness of the original group catalog. Second, we have implicitly assumed that the number of galaxies is conserved. Certainly in the case of morphological transformation, galaxy merging is a possible physical mechanism. It could well be that the merger of two late-type galaxies would produce only one early-type, and the implied change in the late-type fraction would then be smaller than if two early-type galaxies had been produced, leading to an underestimate in the transformation rate as defined in Equation (9). Against these, it should be remembered that the "infall correction," which also accounts for the appearance of new groups with time, will be a worst case scenario, because it assumes that the new group galaxies are drawn randomly from the earlier non-group population.

The derived transformation rates are of course closely linked to the mass functions given above (Figure 7). In particular, given the existence of the transition or crossing mass (where the population is split equally between the two types), and the evidence for the change of this with epoch, we would expect to see the highest transformation rates for galaxies around this same mass $\log(M_*/M_{\odot}) \sim 10.5 \pm 0.5$. At higher masses the transformation rates are lower because the population has saturated with most transformations completed, more than compensating for the small number of potential progenitor galaxies. At lower stellar masses, $\log(M_*/M_{\odot}) \lesssim 10$, not presently accessible by the zCOSMOS observations, the transformation rates must drop again because the vast majority of galaxies are still in the pre-transformation state.

The effect of the environment modifying the transformation rates for star formation activity and color is larger than the environment's effect on the morphological rates, and we conclude that the environment seems to be more closely related to the star formation and color transformation processes than to the

morphological transformation of galaxies. Similar conclusions have been obtained at $z \sim 0$ when using much less direct diagnostics of the environmental influence (e.g., Kauffmann et al. 2004; Blanton et al. 2005; Skibba et al. 2009). For example, Blanton et al. (2005) and Skibba et al. (2009) show that galaxies of the same color do not have significant residual environmental dependence, while colors of galaxies of a given (similar) morphology still show environmental dependence.

This work has clearly demonstrated that, whatever physical processes are involved in the general transformations that are occurring in the galaxy population since $z \sim 1$, especially around the transition or crossing mass, these processes are evidently much more effective in groups than outside of them. The transformation rate outside of groups is by no means zero, but might be lower than we have estimated because of residual contamination of the non-group population by group galaxies, as discussed above.

Our physical interpretation of the shorter timescales that we attribute to the color and/or star formation transitions, compared with those of the morphological transformations, is hindered by the uncertainty about whether the timescales involved are the physical timescales of the transitions (i.e., where $t_p \sim t_\eta$), or what we have called the statistical timescales (where $t_p \ll t_s \sim t_\eta$), as discussed in Section 1. If dealing with prompt phenomena which have the same physical timescale, e.g., say the merging of galaxies, then we would want to interpret the difference in terms of different rates of this event, e.g., different merger rates. On the other hand, in the case of longer term processes, such as strangulation, the difference would be more naturally interpreted in terms of the speed with which the given process acts. Regardless, the fact that the transformation timescales vary rather strongly with galactic mass and with group/non-group environment, and also, but less strongly, with transition type, points toward a picture where a variety of physical processes may be operating.

The current sampling in the 10k zCOSMOS is about ∼30% on average, which is not sufficient to meaningfully split the population of the group galaxies into central and satellite galaxies, because two-thirds of the central galaxies will not have been observed spectroscopically. This will be much easier as the spectroscopic completeness doubles in the final 20k sample, especially if we also use the high quality photometric redshifts. Comparison with the mock group catalog (Knobel et al. 2009) suggests that both group and non-group samples (defined using $M_B < -20.5 - z$) are dominated by central galaxies.

6. CONCLUSIONS

We have used the sample of ∼8500 zCOSMOS galaxies with reliable and accurate spectroscopic redshifts (uncertainty ∼110 km s^{-1}) to study and compare the evolution of galaxies in $0.1 < z < 1$ within and outside group environments.

We have first specifically studied the role of group environment in the morphological transformation of galaxies. We have measured the evolution of the morphological mix of galaxies (split into two broad types: early and late) for well-defined sets of luminosity- and mass-complete samples of galaxies and groups.

1. In the luminosity-complete samples, the fraction of early-type galaxies is higher for galaxies with higher B-band magnitudes. There is a systematic increase in the fraction of early-type galaxies in the group and field environment since $z = 1$. The build-up of the early-type population depends on M_B and environment: brighter early-type galaxies are formed before the fainter early-type galaxies, while early-type galaxies of a given B-band magnitude appear earlier in the group than in the field environment.
2. There is some indication within the group population that the fraction of early types increases with the group richness and velocity dispersion, at least at redshifts $z < 0.65$ and for $M_B < -19.5 - z$.
3. Mirroring the analysis in Bolzonella et al. (2009), the stellar mass function exhibits a different shape for samples of galaxies in different environments (groups, field, and isolated) at least up to $z \sim 0.7$. The stellar mass function shows an upturn at low masses and redshifts in the group environment and more massive galaxies preferentially reside in the groups. The characteristic shape of the stellar mass functions in the group or for the isolated galaxies reflects the different relative contributions of galaxies of different types (e.g., early and late) in different environments. Due to this mass function difference, the environmental effect on galaxy properties must be examined in narrow bins of stellar mass.
4. Looking at narrow mass bins, there is again a systematic build-up of early-type galaxies with stellar masses below $\sim 10^{11}\ M_\odot$ since $z = 1$. At a given cosmic time, the fraction of early-type galaxies in a given environment increases with stellar mass ("morphological downsizing"). For galaxies with masses below $\sim 10^{11}\ M_\odot$, the fraction of early-type galaxies (at a given stellar mass) is always higher in the group than in the field environment, which is higher still than for isolated galaxies. Galaxies with masses above $\sim 10^{11}\ M_\odot$ show little evolution since $z = 1$, having a roughly constant fraction of early-types of ∼0.7−0.8 in both the group and field environments.
5. The build-up of early-type galaxies, as quantified by the "crossing mass" (where the population is split equally between early- and late-type galaxies), shifts to lower stellar masses as cosmic time passes. There is a clear environmental dependence of the rate of change in the crossing mass, such that, at fixed stellar mass, the type transformation happens first for the population of group galaxies, and then for the field galaxies. As time progresses, the crossing mass for morphology diverges between the environments. At $z \sim 0.5$, the net effect of the group environment is equivalent to about 0.2 dex in stellar mass, or 2 Gyr in cosmic epoch.

Broadening our analysis to directly compare the normalized transition rates in morphology with those involving galaxy color and star formation activity, we find the following additional points:

6. The normalized transformation rates are systematically higher in the groups than outside, by a factor of ∼2 or, correcting for infall and the appearance of new groups, by a factor of up to ∼3–4. The rates reach values, for masses around the crossing mass $10^{10.5}\ M_\odot$, as high as 0.3–0.7 Gyr^{-1} in the groups, implying transformation timescales of 1.4–3 Gyr, compared with less than 0.2 Gyr^{-1}, i.e., timescales >5 Gyr, outside of groups.
7. In the group environment, the transformation rates clearly decrease with stellar mass above $10^{10.5}\ M_\odot$, and we infer they must also drop at the lower masses below $10^{10}\ M_\odot$ that are not presently accessible by our spectroscopic data.
8. The transformation rates are consistently higher, by about 50%, for those transformations involving star formation

and color, than for those involving morphological changes. Although these rate/timescale differences are not trivial to interpret (mostly because of uncertainties in the physical processes involved), they suggest faster star formation quenching than morphological transformation, and indicate a tighter relation between the environment and star-formation related processes than between the environment and morphology-related dynamical processes.

9. A clear and important conclusion is that, whatever their physical origin, those transformational processes which have driven the evolution of the galaxy population (around the characteristic transition or crossing mass of $10^{10.5}\ M_{\odot}$) since $z \sim 1$, occur faster, or more efficiently, in the group environment, by a factor of order 3. Although the transformation rate is not zero outside of groups, this suggests that the group environment has played a very significant role in driving the evolution of the overall population.

The next step in the analysis will involve the forthcoming higher sampled 20k zCOSMOS catalog. This will not only increase the group sample by a factor of 2.5 or so, but will also allow (together with improved photo-z) a much better discrimination between the central and satellite galaxies within the groups themselves. This will allow a more direct study of their properties (e.g., morphologies, colors, star formation rates) which will put a stronger constrain on the transformation mechanisms—both the type of processes and their timescales. Ultimately, this will provide an answer as to whether the life paths of a galaxy are really different depending on whether that galaxy is central or a satellite (e.g., Bower et al. 2006; Croton et al. 2006), or if the differences between the centrals and satellites should be more gradual (e.g., Simha et al. 2009).

This work has been supported in part by a grant from the Swiss National Science Foundation and by grant ASI/COFIS/WP3110I/026/07/0.

REFERENCES

Baldry, I. K., Balogh, M. L., Bower, R. G., Glazebrook, K., Nichol, R. C., Bamford, S. P., & Budavari, T. 2006, MNRAS, 373, 469
Balogh, M. L., & Morris, S. L. 2000, MNRAS, 318, 703
Bamford, S. P., et al. 2009, MNRAS, 393, 1324
Barnes, J. E. 1988, ApJ, 331, 699
Bell, E. F., et al. 2004, ApJ, 608, 752
Benson, A. J., Frenk, C. S., Baugh, C. M., Cole, S., & Lacey, C. G. 2001, MNRAS, 327, 1041
Blanton, M. R., Eisenstein, D., Hogg, D. W., Schlegel, D. J., & Brinkmann, J. 2005, ApJ, 629, 143
Bolzonella, M., et al. 2009, arXiv:0907.0013
Boselli, A., & Gavazzi, G. 2006, PASP, 118, 517
Bower, R. G., Benson, A. J., Malbon, R., Helly, J. C., Frenk, C. S., Baugh, C. M., Cole, S., & Lacey, C. G. 2006, MNRAS, 370, 645
Bruzual, G., & Charlot, S. 2003, MNRAS, 344, 1000
Bundy, K., et al. 2006, ApJ, 651, 120
Calzetti, D., Armus, L., Bohlin, R. C., Kinney, A. L., Koornneef, J., & Storchi-Bergmann, T. 2000, ApJ, 533, 682
Capak, P., Abraham, R. G., Ellis, R. S., Mobasher, B., Scoville, N., Sheth, K., & Koekemoer, A. 2007a, ApJS, 172, 284
Capak, P., et al. 2007b, ApJS, 172, 99
Caputi, K. I., et al. 2009, ApJ, 691, 91
Carlberg, R. G., Yee, H. K. C., Morris, S. L., Lin, H., Hall, P. B., Patton, D. R., Sawicki, M., & Shepherd, C. W. 2001, ApJ, 552, 427
Cassata, P., et al. 2007, ApJS, 172, 270
Chabrier, G. 2003, PASP, 115, 763
Cowie, L. L., Songaila, A., Hu, E. M., & Cohen, J. G. 1996, AJ, 112, 839
Croton, D. J., et al. 2006, MNRAS, 365, 11
Cucciati, O., et al. 2010, submitted
Cucciati, O., et al. 2009, arXiv:0911.3740
Davis, M., et al. 2003, Proc. SPIE, 4834, 161
Desai, V., et al. 2007, ApJ, 660, 1151
Dressler, A. 1980, ApJ, 236, 351
Dressler, A., et al. 1997, ApJ, 490, 577
Eke, V. R., et al. 2004, MNRAS, 348, 866
Fasano, G., Poggianti, B. M., Couch, W. J., Bettoni, D., Kjærgaard, P., & Moles, M. 2000, ApJ, 542, 673
Feldmann, R., et al. 2006, MNRAS, 372, 565
Gerke, B. F., et al. 2007, MNRAS, 376, 1425
Gunn, J. E., & Gott, J. R. I. 1972, ApJ, 176, 1
Guzzo, L., et al. 2007, ApJS, 172, 254
Haynes, M. P., & Giovanelli, R. 1984, AJ, 89, 758
Heavens, A., Panter, B., Jimenez, R., & Dunlop, J. 2004, Nature, 428, 625
Holden, B. P., et al. 2007, ApJ, 670, 190
Hubble, E. P. 1926, ApJ, 64, 321
Hubble, E. P. 1936, in Realm of the Nebulae, ed. E. P. Hubble (New Haven, CT: Yale Univ. Press)
Ideue, Y., et al. 2009, ApJ, 700, 971
Iovino, A., et al. 2010, A&A, 509, 40
Kauffmann, G. 1995, MNRAS, 274, 161
Kauffmann, G., White, S. D. M., Heckman, T. M., Ménard, B., Brinchmann, J., Charlot, S., Tremonti, C., & Brinkmann, J. 2004, MNRAS, 353, 713
Kauffmann, G., et al. 2003, MNRAS, 341, 54
Kitzbichler, M. G., & White, S. D. M. 2007, MNRAS, 376, 2
Knobel, C., et al. 2009, ApJ, 697, 1842
Koekemoer, A. M., et al. 2007, ApJS, 172, 196
Kovač, K., et al. 2009, arXiv:0910.0004
Kovač, K., et al. 2010, ApJ, 708, 505
Larson, R. B., Tinsley, B. M., & Caldwell, C. N. 1980, ApJ, 237, 692
Le Fèvre, O., et al. 2005, A&A, 439, 845
Lilly, S. J., et al. 2007, ApJS, 172, 70
Lilly, S. J., et al. 2009, ApJS, 184, 218
Moore, B., Lake, G., & Katz, N. 1998, ApJ, 495, 139
Noordermeer, E., van der Hulst, J. M., Sancisi, R., Swaters, R. A., & van Albada, T. S. 2005, A&A, 442, 137
Poggianti, B. M., et al. 2006, ApJ, 642, 188
Poggianti, B. M., et al. 2009, ApJ, 697, 137
Postman, M., & Geller, M. J. 1984, ApJ, 281, 95
Postman, M., et al. 2005, ApJ, 623, 721
Pozzetti, L., et al. 2009, arXiv:0907.5416
Quilis, V., Moore, B., & Bower, R. 2000, Science, 288, 1617
Rasmussen, J., Ponman, T. J., & Mulchaey, J. S. 2006, MNRAS, 370, 453
Sánchez-Blázquez, et al. 2009, A&A, 499, 47
Sandage, A. 1961, in The Hubble Atlas of Galaxies (Washington, DC: Carnegie Institution)
Scarlata, C., et al. 2007, ApJS, 172, 406
Scoville, N., et al. 2007a, ApJS, 172, 38
Scoville, N., et al. 2007b, ApJS, 172, 150
Silverman, J. D., et al. 2009, ApJ, 695, 171
Simha, V., Weinberg, D. H., Dave, R., Gnedin, O. Y., Katz, N., & Keres, D. 2009, MNRAS, 399, 650
Skibba, R. A., et al. 2009, MNRAS, 399, 966
Smith, G. P., Treu, T., Ellis, R. S., Moran, S. M., & Dressler, A. 2005, ApJ, 620, 78
Tasca, L. A. M., et al. 2009, A&A, 503, 379
Toomre, A., & Toomre, J. 1972, ApJ, 178, 623
van der Wel, A., & van der Marel, R. P. 2008, ApJ, 684, 260
Vergani, D., et al. 2010, A&A, 509, 42
White, S. D. M., et al. 2005, A&A, 444, 365
Wilman, D. J., Balogh, M. L., Bower, R. G., Mulchaey, J. S., Oemler, A., Carlberg, R. G., Morris, S. L., & Whitaker, R. J. 2005, MNRAS, 358, 71
Wilman, D. J., Oemler, A., Mulchaey, J. S., McGee, S. L., Balogh, M. L., & Bower, R. G. 2009, ApJ, 692, 298
Wolf, C., et al. 2009, MNRAS, 393, 1302
Zucca, E., et al. 2009, A&A, 508, 1217